

A lower and more constrained estimate of climate sensitivity

R. B. Skeie et al.

A lower and more constrained estimate of climate sensitivity using updated observations and detailed radiative forcing time series

R. B. Skeie¹, T. Berntsen^{1,2}, M. Aldrin³, M. Holden³, and G. Myhre¹

¹Center for International Climate and Environmental Research – Oslo (CICERO), Oslo, Norway

²Department of Geosciences, University of Oslo, Oslo, Norway

³Norwegian Computing Center, Oslo, Norway

Received: 25 June 2013 – Accepted: 2 July 2013 – Published: 14 August 2013

Correspondence to: T. Berntsen (t.k.berntsen@geo.uio.no)

Published by Copernicus Publications on behalf of the European Geosciences Union.

Title Page

Abstract

Introduction

Conclusions

References

Tables

Figures



Back

Close

Full Screen / Esc

Printer-friendly Version

Interactive Discussion



Abstract

The equilibrium climate sensitivity (ECS) is constrained based on observed near-surface temperature change, changes in ocean heat content (OHC) and detailed radiative forcing (RF) time series from pre-industrial times to 2010 for all main anthropogenic and natural forcing mechanism. The RF time series are linked to the observations of OHC and temperature change through an energy balance model and a stochastic model, using a Bayesian approach to estimate the ECS and other unknown parameters from the data. For the net anthropogenic RF the posterior mean in 2010 is 2.1 W m^{-2} with a 90 % credible interval (C.I.) of 1.3 to 2.8 W m^{-2} , excluding present day total aerosol effects (direct + indirect) stronger than -1.7 W m^{-2} . The posterior mean of the ECS is 1.8°C with 90 % C.I. ranging from 0.9 to 3.2°C which is tighter than most previously published estimates. We find that using 3 OHC data sets simultaneously substantially narrows the range in ECS, while using only one set and similar time periods can produce comparable results as previously published estimates including the heavy tail in the probability function. The use of additional 10 yr of data for global mean temperature change and ocean heat content data narrow the probability density function of the ECS. In addition when data only until year 2000 is used the estimated mean of ECS is 20 % higher. Explicitly accounting for internal variability widens the 90 % C.I. for the ECS by 60 %, while the mean ECS only becomes slightly higher.

1 Introduction

To link long-term targets of climate policy, e.g. the 2°C target (UNFCCC, 2009, 2010), to more specific emission mitigation policy, a key question in climate science is to quantify the sensitivity of the climate system to perturbation in the radiative forcing (RF). The equilibrium climate sensitivity (ECS) is defined as the global mean surface temperature change following a doubling of the CO_2 concentration when the system has reached a new equilibrium. However, the ECS has been poorly constrained, with

ESDD

4, 785–852, 2013

A lower and more constrained estimate of climate sensitivity

R. B. Skeie et al.

Title Page

Abstract

Introduction

Conclusions

References

Tables

Figures



Back

Close

Full Screen / Esc

Printer-friendly Version

Interactive Discussion



A lower and more constrained estimate of climate sensitivity

R. B. Skeie et al.

Title Page

Abstract

Introduction

Conclusions

References

Tables

Figures



Back

Close

Full Screen / Esc

Printer-friendly Version

Interactive Discussion



significant probabilities for high values. The ECS was given a likely (> 66 % probability) range of 2 to 4.5 °C with a best estimate of 3 °C by the Intergovernmental Panel on Climate Change (IPCC, 2007) and values substantially higher than 4.5 °C could not be excluded. For constraining the ECS there are two main approaches. A “bottom up” approach performing Monte Carlo simulations or multi-model experiment with General Circulation Models (GCMs) (Andrews et al., 2012; Murphy et al., 2004; Piani et al., 2005; Stainforth et al., 2005) and a “top down” approach constraining the ECS using RF estimates and observed data on past climate change on various timescales: the 20th century warming (Andronova and Schlesinger, 2001; Annan and Hargreaves 2006; Forest et al., 2002, 2006, 2008; Frame et al., 2005; Gregory et al., 2002; Knutti et al., 2002; Meinshausen et al., 2009; Tomassini et al., 2007; Libardoni and Forest, 2011; Huber and Knutti, 2012; Olson et al., 2012; Otto et al., 2013; Lewis et al., 2013; Ring et al., 2013), last millennium using proxy data (Hegerl et al., 2006), last glacial maximum (Annan et al., 2005; Schneider von Deimling et al., 2006) or using data further back in time (Hansen and Sato, 2012; Kohler et al., 2010; Royer et al., 2007).

The main challenge in determining the climate sensitivity is that it is governed by complex feedback mechanisms. Bottom-up estimates use prescribed CO₂ perturbations (i.e. the RF known with small uncertainty), but the uncertainties in the representation of the physics and thus the feedbacks lead to large uncertainties in the ECS (Andrews et al., 2012). For the top-down approach the Earth can be considered as a “laboratory” in which all feedbacks are by definition perfectly represented, although the impact of very slow feedbacks like melting of ice caps might not be fully captured. The problem is that the human induced “climate experiment” is not very well set up in that neither the RF nor the response is well known. There is a combination of positive and negative contributions and the documentation of the changes in the system is less than perfect. However, this is an ongoing experiment and over time the net positive forcing increase as CO₂ continues to increase while the concentrations of scattering aerosols have more or less stabilized (Skeie et al., 2011; Wild et al., 2009). Our understanding of the physics and magnitude of the forcings (e.g. the aerosol forcings)

A lower and more constrained estimate of climate sensitivity

R. B. Skeie et al.

Title Page

Abstract

Introduction

Conclusions

References

Tables

Figures



Back

Close

Full Screen / Esc

Printer-friendly Version

Interactive Discussion



have also improved leading to less uncertainty in the RF estimates (Myhre, 2009), and the time series of observations become longer and with improved quality. This combination is expected to provide a better constraint on the ECS. Estimating the climate sensitivity using historical data implicitly assumes that the feedbacks do not change over time, which is equivalent to assuming that the effective climate sensitivity (Frame et al., 2005; Murphy, 1995) and the ECS are equal. This assumption adds some additional uncertainty to the estimate of the tail of the ECS towards higher values, since the slow feedbacks are not fully represented. However, these changes are slow and the climate sensitivity estimated here (i.e. the average effective climate sensitivity over the 1750–2010 period) is what is required for analysis of climate change on a century timescale (Raper et al., 2001; Sokolov et al., 2003).

In this study, RF time series with uncertainty of all well-established mechanisms are linked to the observations of ocean heat content (OHC) and temperature change through an energy balance model and a stochastic model, using a Bayesian approach to estimate the climate sensitivity following the method described in Aldrin et al. (2012), but with certain improvements (Sect. 2). Observational data up to and including year 2010 are used. This is at least ten additional years compared to the majority of previously published studies (Hegerl et al., 2007; Knutti and Hegerl, 2008). A key feature of both the near-surface air temperatures and the OHC is an apparent flattening during the last decade (Easterling and Wehner, 2009; Palmer et al., 2010). Thus the situation over the last decade with the possibility for better quantification of the net RF and more observations can give significant new information.

A Bayesian statistical approach also provides posterior estimates of all RF mechanisms and an estimate of the magnitude and time scales of unforced natural variability in the system. The ECS probability density function (PDF) with a heavy tail has recently been discussed (Frame et al., 2005; Fiore et al., 2009; Hannart et al., 2009; Roe and Baker, 2007; Roe and Armour, 2011; Annan and Hargreaves, 2011) and Allen and Frame (2007) called off the quest for finding the upper bound of the ECS. In the recent years, the transient climate response (TCR, defined as the global mean temperature

A lower and more constrained estimate of climate sensitivity

R. B. Skeie et al.

[Title Page](#)[Abstract](#)[Introduction](#)[Conclusions](#)[References](#)[Tables](#)[Figures](#)[⏪](#)[⏩](#)[◀](#)[▶](#)[Back](#)[Close](#)[Full Screen / Esc](#)[Printer-friendly Version](#)[Interactive Discussion](#)

change at the time of CO₂ doubling under a scenario of 1 %yr⁻¹ increase in CO₂) has therefore received more attention (Stott and Forest, 2007; Gregory and Forster, 2008; Forest et al., 2008; Knutti and Tomassini, 2008; Padilla et al., 2011; Stott et al., 2006). The TCR is non-linearly related to ECS (Allen et al., 2000). The ECS temperature response will eventually be realized on a timescale on century to millennia when the system has reached a new equilibrium. The uncertainty in TCR may therefore be more relevant for near-term transient climate change (Cubasch et al., 2001; Hegerl et al., 2007). Based on the updated model we also present a PDF for the TCR.

2 Methods

2.1 The model

The core of our model framework is a deterministic energy balance model (EBM) (Schlesinger et al., 1992), which calculates annual hemispheric- and global mean near-surface temperature change and changes in global ocean heat content (OHC) as a function of estimated RF time series. The ECS is an explicit parameter in the EBM and can therefore be constrained in a Bayesian framework. The deterministic model is combined with a stochastic model and fitted to observations of annual hemispheric mean temperature change and OHC. The ECS is given a vague prior, uniform [0, 20] °C, while the other model parameters and the RF time series are given informative priors based on expert judgment. The EBM and the choice of priors are described in Appendix A and Aldrin et al. (2012).

The EBM does not capture internal natural variability in the climate system, such as the El Niño–Southern Oscillation (ENSO). In the stochastic model we account for the effect of ENSO using the Southern Oscillation index. Also on multi-decadal scales there may be internal natural variability (e.g. Hegerl et al., 2007). This is taken into account by an explicit term for long-term variability. To represent the real world, an error term is included in the stochastic model accounting for model errors due to limitations of

the EBM and forcing time series. Finally, another error term is included to account for observational errors. The model can then be written

$$\mathbf{y}_t = \mathbf{m}_t(\mathbf{x}_{1750:t}, \text{ECS}, \boldsymbol{\theta}) + \boldsymbol{\beta}_1 e_t + \mathbf{n}_t^{\text{liv}} + \mathbf{n}_t^{\text{m}} + \mathbf{n}_t^{\text{o}}. \quad (1)$$

Here, \mathbf{y}_t is a vector with observations for year t . The first six elements are hemispheric temperature estimates from three different data sets (see below). The last three elements are estimates of OHC in the upper 700 m, from three OHC data sets (see below). The $\mathbf{m}_t(\mathbf{x}_{1750:t}, \text{ECS}, \boldsymbol{\theta})$ is the EBM with RF time series from 1750 until year t ($\mathbf{x}_{1750:t}$) as input, and the ECS as a parameter in addition to other physical parameters ($\boldsymbol{\theta}$). The output from $\mathbf{m}_t(\cdot, \cdot, \cdot)$ are the hemispheric temperatures and the OHC, copied three times to match the observations, which is the case also for $\boldsymbol{\beta}_1 e_t$, $\mathbf{n}_t^{\text{liv}}$ and \mathbf{n}_t^{m} .

The e_t is the Southern Oscillation index (<http://www.bom.gov.au/climate/current/soihtm1.shtml>, Bureau of Meteorology, Australia) and $\boldsymbol{\beta}_1$ is a coefficient vector with one value for each hemisphere, and which is 0 for OHC. The two coefficients are estimated from the data.

The long-term internal variability is represented by the term $\mathbf{n}_t^{\text{liv}}$. The dependence structure of this term is based on control simulations with GCMs from CMIP5 (Appendix A). This gives us an estimate of the internal variability from an external data source. In the main analysis the Canadian ESM (CanESM2) is used, however, in a separate sensitivity test the Norwegian ESM (NorESM) is used. The term \mathbf{n}_t^{m} is the model error, while \mathbf{n}_t^{o} is the observational error. Both these terms are modeled as a vector autoregressive model of order 1 (Appendix A).

Note that the standard deviations of all stochastic terms are treated as unknowns and are estimated from the data, which insures that the modelled variance on the right side of Eq. (1) is consistent with the variance of the data. This differs from the approach of Meinshausen et al. (2009) or Huber and Knutti (2012), who's model contain some of the same stochastic terms, but where all variances are kept fixed to values based on external sources.

A lower and more constrained estimate of climate sensitivity

R. B. Skeie et al.

Title Page

Abstract

Introduction

Conclusions

References

Tables

Figures

◀

▶

◀

▶

Back

Close

Full Screen / Esc

Printer-friendly Version

Interactive Discussion



the 90 % uncertainty range for year 2010. The uncertainty ranges for the anthropogenic RF are based on Fig. 1d in Skeie et al. (2011) (Appendix C). Separate RF-time series for each hemisphere are used as input to the EBM (Appendix C).

We also include forcing mechanisms that are not strictly radiative forcings according to the IPCC AR4 (i.e. the cloud lifetime and the semi-direct effects) since they act much more rapid than the time scale of global surface temperature change (Lohmann et al., 2010). We include the semi-direct effect as a uniform distribution of -0.25 to $+0.50 \text{ W m}^{-2}$ in 2007 (Isaksen et al., 2009), assuming it is proportional to the RF of black carbon (BC) from contained combustion.

For the total direct aerosol effect the uncertainty is better constrained for the recent years utilizing both models and satellites (Myhre, 2009). We adopt the same relative uncertainty as in Forster et al. (2007) for each aerosol component, but the standard deviation for each component is multiplied by a factor for the years 2000–2010 to match the total direct aerosol effect uncertainty in Skeie et al. (2011). The factor increases linearly back in time reaching 1.0 in 1950 and being constant thereafter (Appendix D). For the other components we assume the same relative uncertainty for all years, except otherwise stated in Table 1.

We use the common assumption that the RF mechanisms are additive and independent (Boucher and Haywood, 2001). The prior distributions for the RF time series are shown in Fig. 1. The mean value for the anthropogenic RF in 2010 is 1.5 W m^{-2} with a 90 % C.I. of 0.27 to 2.5 W m^{-2} . The mean value is weaker than the mean value of the net anthropogenic RF in IPCC AR4 of 1.6 W m^{-2} (Forster et al., 2007), and our prior is wider. This is reasonable since the RF the IPCC estimate did not include the cloud lifetime and the semi-direct effects. The prior for the total aerosol effect, which include the direct effect, the cloud albedo effect, the cloud lifetime effect and the semi-direct effect, has a mean value of -1.5 W m^{-2} in 2010 and a 90 % C.I. of -2.7 to -0.63 W m^{-2} .

ESDD

4, 785–852, 2013

A lower and more constrained estimate of climate sensitivity

R. B. Skeie et al.

Title Page

Abstract

Introduction

Conclusions

References

Tables

Figures



Back

Close

Full Screen / Esc

Printer-friendly Version

Interactive Discussion



3 Results

In this section we present the results of our analysis where the parameter values in the EBM are updated using observations of hemispheric temperature and OHC (0–700 m) to year 2010 and detailed RF time series from 1750 to 2010 (the main analysis).

We investigate the effect the last 10 yr of observational data have on the estimated ECS, and calculate PDFs of the TCR using the joint posterior distribution of the model parameters.

3.1 Main analysis

The posterior RF time series and PDFs for RF in 2010 are shown in Fig. 1. The posterior mean of the total RF is higher than the prior mean (Fig. 1 upper panel) mainly due to the weakening of the total aerosol effect when the model is updated with data (Fig. 1 lower panel). In the mid-20th century (1940s–1970s) the posterior mean of the total anthropogenic RF time series show much weaker change compared to the decreasing RF for the prior assumptions (Fig. 1 middle panel). In this period the observed global mean temperature shows a slight cooling (Trenberth et al., 2007). Our analysis suggests that the net anthropogenic RF did not cause such a global cooling. This is in accordance with Thompson et al. (2010) that related the decrease in the observed temperature between 1940s to 1970s to two distinct periods. The first one was a discontinuity in the mid-1940s, due to uncorrected instrumental biases in the sea surface temperature (SST) (Thompson et al., 2008). The second period was around 1970 when an abrupt drop in Northern Hemisphere SST was observed which is real and not related to any instrumental bias. The bias in the mid-1940s is not corrected in the surface temperature data used. A sensitivity test replacing HadCRUT3 with HadCRUT4 (Morice et al., 2012) which includes this SST correction has been carried out and gave almost identical results (Fig. 2c vs. 2a).

The posterior RF for the total aerosol effect is weaker than the prior assumptions (Fig. 1) with a mean posteriori value in 2010 of -1.06 W m^{-2} and a 90 % C.I. of -1.7 to

ESDD

4, 785–852, 2013

A lower and more constrained estimate of climate sensitivity

R. B. Skeie et al.

Title Page

Abstract

Introduction

Conclusions

References

Tables

Figures

◀

▶

◀

▶

Back

Close

Full Screen / Esc

Printer-friendly Version

Interactive Discussion



-0.40 W m^{-2} . Previous studies (Andronova and Schlesinger, 2001; Forest et al., 2002) have highlighted the role of the inter-hemispheric temperature difference as a key diagnostic to determine the aerosol forcing. Our approach which includes hemispheric RF and temperature data, and models the hemispheric temperatures separately, implicitly takes this into account. The EBM used here accounts for different ocean volumes due to different land fractions in the two hemispheres, thereby imposing a different effective heat capacity and thus a different temporal response to short-term RF changes in the two hemispheres. In our main analysis we do not allow for hemispheric differences in the climate sensitivity parameter. Other EBMs (e.g. Raper et al., 2001) have imposed a fixed hemispheric difference in the climate sensitivity parameter to emulate the response of specific GCMs. In a sensitivity tests we have allowed for hemispheric differences in the climate sensitivity parameter (cf. Sect. 4.4). Based on inverse estimates of net aerosol RF over the 20th century, that are consistent with observed warming, Hegerl et al. (2007) gave a similar likely range of -1.7 to -0.1 W m^{-2} . The range in IPCC AR4 based on climate models for the sum of all aerosol effects was broader, -2.3 to -0.2 W m^{-2} (Denman et al., 2007). Our result is in accordance to the residual forcing (all aerosol effects and any unknown mechanisms) found by Murphy et al. (2009). They found a residual RF of $-1.1 \pm 0.4 \text{ W m}^{-2}$ (1σ), corresponding to a 90 % C.I. of -1.8 to -0.44 W m^{-2} , between pre-industrial and the 1970–2000 period. This is similar to the total aerosol RF posterior mean of -1.12 W m^{-2} (90 % C.I. of -1.7 to -0.53 W m^{-2}) for the 1970–2000 average in our analysis.

A strong historical aerosol cooling implies a high ECS to be consistent with observed temperature trend (Andreae et al., 2005). Our results show a weaker aerosol forcing than our prior assumption, and the ECS posteriori mean is 1.8°C (Fig. 2a) which is below the lower limit of the likely range ($> 66\%$ probability) for the ECS of 2 to 4.5°C in IPCC AR4 (Meehl et al., 2007). The 90 % C.I. of the posterior ECS is 0.9 to 3.2°C , and the heavy upper tail often seen in estimates of ECS is less pronounced. The probability of ECS being larger than the upper limit of the IPCC likely range of 4.5°C is 0.014 . Tomassini et al. (2007), who used observational data up to 2003, found a probability of

A lower and more constrained estimate of climate sensitivity

R. B. Skeie et al.

Title Page

Abstract

Introduction

Conclusions

References

Tables

Figures

◀

▶

◀

▶

Back

Close

Full Screen / Esc

Printer-friendly Version

Interactive Discussion



A lower and more constrained estimate of climate sensitivity

R. B. Skeie et al.

Title Page

Abstract

Introduction

Conclusions

References

Tables

Figures

◀

▶

◀

▶

Back

Close

Full Screen / Esc

Printer-friendly Version

Interactive Discussion



0.16 for the ECS $> 4.5^\circ\text{C}$. We have used observational data up through 2010, seven more years than Tomassini et al. (2007). Recently, Hansen and Sato (2012) stated that the ECS is $3 \pm 1^\circ\text{C}$ (1σ) based on climate oscillations over the last 800 000 yr, corresponding to a 90 % C.I. of 1.4 to 4.6°C . Another recent study found a lower value for the ECS with a 90 % C.I. of 1.4 to 2.8°C (Schmittner et al., 2011) using data from the last glacial maximum.

The fitted posterior mean and the observed hemispheric temperatures and OHC are compared in Fig. 3. For the SH and for the OHC, the model is reproducing the long-term trend of the observations. In the NH, the fitted temperature increase over the last two decades is not as rapid as in the observations, leaving the observations just outside to 90 % C.I. of the fitted temperatures. The 90 % C.I. shown in the figure accounts only for the uncertainty in the deterministic terms at the right side of Eq. (1), i.e. of $m_t(x_{1750:t}, \text{ECS}, \theta) + \beta_1 e_t$, so we cannot expect that the 90 % of observations lies within these limits. Much of the discrepancies are accounted for by the long-term internal variability represented by the term n_t^{liv} (Fig. 4). This figure shows also the posterior estimates for the ENSO term $\beta_1 e_t$ and the model error n_t^m . Figure 4 is discussed further in Sect. 4.3.

3.2 Updating model with data between year 2000 and 2010

Our 90 % C.I. for ECS is tighter compared to previous estimates of the ECS. To investigate how much information that is obtained over the last 10 yr, we have re-estimated the model using only data up to year 2000. The resulting posterior distribution of ECS is shown in Fig. 2f. Furthermore, the model is updated sequentially with 2 yr of additional data between 2000 and 2010. Figure 5 shows the sequence of estimated ECS with 90 % C.I. and the relative uncertainty R90. The R90 values are steadily decreasing, except from 2002 to 2004, as we add more data showing the value of a longer time series in constraining the ECS estimate. The ECS estimate itself, however, is shifted slightly towards higher values when the model is updated with data from 2003 and 2004, and when the model is further updated with data from 2005 and 2006 the ECS estimate

is still the second highest of these six estimates. The reason is probably that the RF (both prior and posterior) remains at the same level between 2002 and 2006, whereas the OHC increases, especially between 2002 and 2004. After 2006, the RF increases again, while there is little or no increase in the OHC.

The drastic reduction in uncertainty (R90 reduced from 2.20 to 1.23) with ten more years of data may be surprising. We believe there are two main reasons for this. First, the RF increased significantly in this period, so these ten years of data are more informative than data from a period of same length, but with less variation in RF. Second, while the temperature series is lengthened by 6–8%, the OHC series are extended by about 20%. Since the OHC data are more informative, ten years of data gives therefore an important contribution to the information content in the data.

3.3 Transient climate response

To determine a PDF for the TCR the EBM is run with a 1% per year increase in CO₂ using the joint posterior distribution of the model parameters. The TCR from the main analysis has a posterior mean estimate of 1.4°C and a 90% C.I. of 0.79 to 2.2°C, while using the model parameters constrained by data only up to year 2000 give a wider distribution with a 90% C.I. of 0.54 to 2.9°C. Recently, Padilla et al. (2011) also found a narrowing of the TCR over the last decade with a 90% C.I. of 1.3 to 2.6°C in 2008. Also Gillett et al. (2012), estimated a narrower range of TCR using observations over the period 1851–2010 than 1900–1999. Our results are in line with other estimates of TCR, (Stott et al., 2006; Knutti and Tomassini, 2008; Gregory and Forster, 2008) and are slightly shifted to weaker values when the model is updated with data up to 2010. GCM model results lead to the conclusion in IPCC AR4 that TCR is very likely larger than 1°C and very unlikely greater than 3°C (Meehl et al., 2007). Our estimate suggests that the TCR lies in the lower range of the IPCC very likely range.

A lower and more constrained estimate of climate sensitivity

R. B. Skeie et al.

Title Page

Abstract

Introduction

Conclusions

References

Tables

Figures



Back

Close

Full Screen / Esc

Printer-friendly Version

Interactive Discussion



4 Discussion

The results from our main analysis show a lower and better constrained estimate of the climate sensitivity compared to the majority of previous estimates. In this section we investigate the role of several factors that would impact the expected value as well as the uncertainty in the estimated climate sensitivity. This includes structural features of the EBM, the uncertainties in the RF and in the surface air temperatures and OHC data, and the role of internal variability. We perform a sensitivity analysis including recent observational data on OHC trends for depths below 700 m.

4.1 Uncertainties in radiative forcing

To constrain the climate sensitivity, the treatment of RF-uncertainties is important. Tanaka et al. (2009) suggested that the probability for high climate sensitivity is even higher than previous estimates because of insufficient handling of the historical development of the RF uncertainty. The uncertainties in the RF time series are simply treated in this study, however more sophisticated than in many previous studies that have used a scaling approach related to only the aerosol RF (Andronova and Schlesinger, 2001; Forest et al., 2006; Gregory et al., 2002; Knutti et al., 2002). We include the uncertainty for all components (Table 1), as in Tomassini et al. (2007) who scaled individually the nine RF mechanisms they considered. The uncertainty in the temporal pattern of each RF mechanism is not included, but the net RF time series will have uncertainty in the temporal structure when all the RF mechanisms are combined.

Since the ECS is better constrained by adding data for the last 10 yr, we first investigate the RF over the last decade. Solomon et al. (2010) explained some of the recent trend in temperature by a reduction in stratospheric H₂O. They calculated a RF of -0.1 W m^{-2} in 2000–2005 relative to 1996–2000. Data before mid-1990s are sparse, but observations indicate an increase between 1980 and 2000, possibly being an important driver for decadal climate change (Solomon et al., 2010). The reason for the recent decrease is not clear, and if the change in stratospheric H₂O is due to natural

ESDD

4, 785–852, 2013

A lower and more constrained estimate of climate sensitivity

R. B. Skeie et al.

Title Page

Abstract

Introduction

Conclusions

References

Tables

Figures

◀

▶

◀

▶

Back

Close

Full Screen / Esc

Printer-friendly Version

Interactive Discussion



A lower and more constrained estimate of climate sensitivity

R. B. Skeie et al.

Title Page

Abstract

Introduction

Conclusions

References

Tables

Figures

◀

▶

◀

▶

Back

Close

Full Screen / Esc

Printer-friendly Version

Interactive Discussion



variability or a climate feedback it should not be included as a RF in our setup. Only changes from CH₄ oxidation are taken into account in our analyses. Stratospheric aerosols have increased since 2000 contributing to -0.1 W m^{-2} (Solomon et al., 2010). Vernier et al. (2011) related this to recent tropical volcanoes. We have used the updated values for stratospheric aerosol optical thickness from Sato et al. (1993) which give a maximum RF of -0.14 W m^{-2} in 2003 and 2005 for volcanic RF. In comparison the net anthropogenic RF increased by 0.42 W m^{-2} over the last decade for our prior assumptions (0.33 W m^{-2} from LLGHGs). In addition the sun experienced a minimum in activity around 2010, and the prior mean solar RF in 2010 relative to the maximum in 2000 is -0.14 W m^{-2} .

Kaufmann et al. (2011) investigated temperature trend during the last decade, and related it mainly to the solar minimum and ENSO, but also to strengthening of the sulfur RF due to increased emissions in China. For our prior RF time series for the direct aerosol effect, the strengthening of the sulfur direct aerosol effect has been offset by the strengthening in the BC direct aerosol effect from 2000 to 2010 (Skeie et al., 2011). The BC effect was not considered by Kaufmann et al. (2011). BC emissions from China, increased by $\sim 20\%$ between 2000 and 2010, in agreement with the inventory by Zhang et al. (2009) where it increased by 13% between 2000 and 2005, but weaker than the 46% increase between 2000 and 2010 from Lu et al. (2011). This inventory also shows an increase of 46% for the sulfur emissions between 2000 and 2010 in agreement with the $\sim 50\%$ increase in Chinese emissions over the same period used in Skeie et al. (2011). To test how the temporal structure of the RF over the last years affect the results we did a sensitivity test (Appendix E). We also tested the sensitivity to changes in the temporal development of the RF early in the simulation period and to the role if uncertain data before 1900 (update with data only between 1900 and 2010 to exclude the uncertain early period including the 1883 Krakatoa volcanic eruption). In both cases the altering of the temporal structure of the prior RF had only very minor effects on the estimated ECS (Fig. E1).

A lower and more constrained estimate of climate sensitivity

R. B. Skeie et al.

Title Page

Abstract

Introduction

Conclusions

References

Tables

Figures



Back

Close

Full Screen / Esc

Printer-friendly Version

Interactive Discussion



There are other proposed RF mechanisms that are not included here due to large uncertainties and lack of scientific understanding, which could possibly alter the ECS estimate. For the indirect aerosol effects we have included the cloud albedo effect, cloud lifetime effect and the semi-direct effect. The prior time series for the indirect effects, constructed in a simple way, are based on aerosol effects on liquid water clouds. Aerosols may influence mixed phased clouds (Denman et al., 2007) and the indirect effect of aerosols on ice clouds are very uncertain, but possibly of great importance (Penner et al., 2009). However, if all indirect effects have a similar temporal pattern, there is a clear signal that the data do not allow large negative values for the total aerosol effect (Fig. 1).

We have assumed that the RF mechanisms have equal temperature response, are additive and independent, which may not be entirely valid. The climate efficacy, that the climate sensitivity depends on the type of forcing (Hansen et al., 2005; Joshi et al., 2003), is not considered. However, we include the semi-direct effect and the cloud lifetime effect as forcings, and these effects are partly reasons for including differences in climate efficacy in GCMs (Forster et al., 2007). There are few studies considering efficacy, and the efficacy for different forcing mechanisms generally lies in the range 0.6 to 1.3 (Forster et al., 2007). The efficacy can be assumed to be partly included in the RF uncertainty, but a proper inclusion of efficacy will increase the uncertainty in the estimated ECS. We have also assumed that the RF errors are independent. This may not be true, since e.g. the forcing mechanisms related to emissions due to fossil fuel use will be dependent. It is also plausible that the magnitudes of the different aerosol effects are related. However, insufficient information is available to include dependent radiative forcing error estimates.

The RF due to CO₂ is calculated based on measured changes in CO₂ concentrations. There is an implicit assumption that any contribution to the historic CO₂ change from climate feedbacks is negligible (Forster et al., 2007). However, (Arora et al., 2009) estimate that as much as 15–20 ppm of the CO₂ increase may be due to climate

feedbacks. Allowing for such a feedback in our analysis would lead to a lower RF estimate and thus a somewhat higher estimate of the climate sensitivity.

4.2 The role of ocean heat content

Previous studies (Tomassini et al., 2007; Urban and Keller, 2009) have shown that OHC data have the potential to constrain the ECS estimate. To test how the OHC data affects the ECS estimate, several sensitivity test are performed (see below and Appendix E).

The Argo floats were introduced in early 2000s greatly improving the ability to estimate OHC (<http://www.argo.ucsd.edu/>). For earlier years the record is spatially inhomogeneous with poor coverage in SH and the main data used were collected from expendable bathythermographs (XBT) which have systematic data errors (Gouretski and Koltermann, 2007). Lyman et al. (2010) found that XBT bias correction was the main source of uncertainty in the warming trend from 1993 to 2008. The OHC data from Levitus et al. (2009) have recently been updated and known biases in both the Argo data and XBT data have been corrected. The fitted OHC from the model is compared with the three historical estimates in Fig. 3. The fitted OHC is a smooth curve compared to the observations that show more inter-annual variability. The fitted OHC curve has dips related to volcanoes as is also seen in the observations.

Lyman et al. (2010) found a linear warming trend of 0.64 W m^{-2} for the period 1993 to 2008, while in the main analysis we found a 1993 to 2008 trend of $0.32 \pm 0.07 \text{ W m}^{-2}$. The trend in Lyman et al. (2010) is larger than the recent updated trends from Levitus et al. (2009) and Church et al. (2011), and both estimates are outside the 90 % confidence interval of 0.53 to 0.75 W m^{-2} presented in Lyman et al. (2010). The difference is mainly prior to 2003 since the estimate of Lyman et al. (2010) and two of the three OHC data sets used in this study show a flattening of the OHC since 2004.

The observed OHC data have been used to close the Earth's energy budget. Murphy et al. (2009) and Church et al. (2011) found a jump in the residual RF in the mid-1990s. The residual RF is the remaining energy flux, allocated primarily to the direct and indirect aerosol effects, after accounting for surface temperature increase, increase in OHC

A lower and more constrained estimate of climate sensitivity

R. B. Skeie et al.

Title Page

Abstract

Introduction

Conclusions

References

Tables

Figures



Back

Close

Full Screen / Esc

Printer-friendly Version

Interactive Discussion



A lower and more constrained estimate of climate sensitivity

R. B. Skeie et al.

Title Page

Abstract

Introduction

Conclusions

References

Tables

Figures



Back

Close

Full Screen / Esc

Printer-friendly Version

Interactive Discussion



and known RF mechanisms when the energy balance is assessed. Church et al. (2011) related the strengthening of the residual forcing in the mid-1990s partly to increased aerosol loading in the developing world, while Murphy et al. (2009) excluded this since observed global aerosol optical depth was constant or slightly declining during the 1990s. Hansen et al. (2011) found that the calculated radiative imbalance was consistent with observations of the energy imbalance, which is largely determined by the observed OHC data. Hansen and Sato (2012) and Loeb et al. (2012) concluded that there is no missing energy in the recent years as was indicated by Trenberth and Fasullo (2010). The inferred planetary energy imbalance from Hansen et al. (2011) was $0.58 \pm 0.15 \text{ W m}^{-2}$ during the 6 yr period 2005–2010 assuming a stronger aerosol RF ($-1.6 \pm 0.3 \text{ W m}^{-2}$) and a larger climate sensitivity ($3 \pm 1.0^\circ\text{C}$) than the posterior means in this study. We find a similar planetary imbalance of $0.46 \pm 0.16 \text{ W m}^{-2}$ over the same time period.

Since the sea level has continued to increase Meehl et al. (2011) explained the recent flattening in the OHC in the upper ocean by an increase in the deep ocean. Meehl et al. (2011) used model simulations, and found that periods with no increase in temperature in the upper ocean are accompanied by an increasing temperature in the deeper ocean. In the 1990s and 2000s Purkey and Johnson (2010) found an increase in OHC in abyssal and deep Southern Ocean based on sparse observations from ships, but it is not clear if it is a long-term trend. Palmer et al. (2011) highlighted the importance of deep ocean observations to monitor the Earth's energy balance. Our main estimate is not constrained by deep ocean data. Between, 1961 to 2010, 11 % of the total increase in OHC occurred below 700 m in the main analysis. Hansen et al. (2011) used 15 % for the period 1993–2008 and 19 % for the period 2005–2010, assuming constant heat uptake in the deep ocean from the work by Purkey and Johnson (2010).

Very recently OHC data for the deeper ocean have become available, for the layer 700–2000 m for the period 1955–2010 (Levitus et al., 2012), and below 3000 m between 1985 and 2006 (Kouketsu et al., 2011). We have made an additional simplified sensitivity test with our model using the 3 OHC datasets for 0–700 m as in the main

A lower and more constrained estimate of climate sensitivity

R. B. Skeie et al.

Title Page

Abstract

Introduction

Conclusions

References

Tables

Figures



Back

Close

Full Screen / Esc

Printer-friendly Version

Interactive Discussion



analysis and the new deep ocean OHC data for the two decades of data and assumed zero change in the deep ocean OHC when no data are available. The sum of these OHC deep ocean trend data is included to constrain the total OHC in our model between 700 m and the ocean floor. Including the deep ocean data leads to an increased mixing of heat down to the deep ocean and a small increase in the estimated ECS (Fig. 2d vs. 2a). For the 2005 to 2010 period the estimated increase in OHC for the entire ocean is $0.37 \pm 0.14 \text{ W m}^{-2}$ for the main analysis and $0.40 \pm 0.16 \text{ W m}^{-2}$ for the sensitivity with data for the deep ocean. This is in good agreement with the heat gain of 0.39 W m^{-2} (averaged over the whole globe) in the upper 1500 m of the ocean estimated by von Schuckmann and Le Traon (2011) based on the ARGO measurement network.

As discussed above, and also demonstrated in the sensitivity tests described in Appendix E (cf. Fig. E1b vs. E1g), the OHC data have the potential to constrain the ECS estimate. However, while the temperature series are quite similar, the three OHC series differs considerably more, indicating that the observational errors for the OHC data can be large (and perhaps larger than some of the data providers report, see Figs. B3 and B4 in Appendix B). Therefore, using three OHC series simultaneously instead of only one should decrease the uncertainty of the ECS estimate due to reduced influence of observational errors. This is demonstrated in a sensitivity test where we use only one OHC data set (from Levitus et al., 2009) and data only up to 2000 as in many previous studies (Fig. 2g). Using 3 OHC datasets, the PDF for the ECS is considerably narrower (Fig. 2f). Using only one OHC dataset the PDF for the ECS is remarkably wider (Fig. 2g), with a posterior mean shifted towards the prior mean (which is 10°C). The 90% C.I. is 1.1 to 14.5°C with a mean value of 4.5°C in line with or even higher than previously published estimates (Andronova and Schlesinger, 2001; Annan and Hargreaves, 2006; Forest et al., 2002, 2006; Frame et al., 2005; Gregory et al., 2002; Knutti et al., 2002; Tomassini et al., 2007) that used observational data for time periods ending between 1994 and 2003. This indicates that the narrow range of the ECS in the main analysis is not due to an artifact of the model used, but indeed due to the

A lower and more constrained estimate of climate sensitivity

R. B. Skeie et al.

Title Page

Abstract

Introduction

Conclusions

References

Tables

Figures



Back

Close

Full Screen / Esc

Printer-friendly Version

Interactive Discussion



added observational information by the two additional OHC datasets and the 10 additional years. In the cases with three and one OHC dataset the posterior distribution of total aerosol effect in 2000 is -1.2 W m^{-2} with a 90% C.I. of -1.9 to -0.59 W m^{-2} , and -1.4 W m^{-2} with a 90% C.I. of -1.9 to -0.71 W m^{-2} , respectively. The estimated total aerosol effects are stronger than in the main analysis that had a mean value of -1.1 W m^{-2} in 2000.

4.3 Multidecadal oscillations

In the North Atlantic the observed SSTs show a multidecadal oscillation, known as the Atlantic Multidecadal Oscillation (AMO) (Kerr, 2000). Whether AMO is due to external forcing or internal variability is however not clear (e.g. Knight, 2009; Ottera et al., 2010). DeIsole et al. (2011) explicitly identified a significant unforced multidecadal component using climate simulations and observations, and found that the AMO is dominated by internal dynamics. Using observed temperature Wu et al. (2011) separated the temperature trend in a secular trend related to fossil fuel emissions and a multidecadal variability. Wu et al. (2011) found a significant contribution to the late 20th century warming from this multidecadal variation.

In the stochastic model multidecadal variability is represented by a separate term (n_t^{liv}) based on results from long control simulations with CanESM2 (main analysis) or NorESM. The difference between the ECS estimates using these two GCMs (Fig. 2b vs. 2a) is minor. To investigate the impact of prior knowledge about the multidecadal variability we have performed a sensitivity test ignoring the explicit term for long-term internal variability (Fig. 2h). In such a simplified model, temporary increasing or decreasing trends in temperature or OHC over 10–20 yr may falsely be accounted as permanent trends, giving too optimistic uncertainty estimates. As expected, adding unforced long-term variability gives a larger uncertainty in the estimated climate sensitivity. Also the expected value becomes somewhat higher (Fig. 2a vs. 2h). This is reasonable since in general larger uncertainty will move the posterior mean towards the

prior mean. The posterior estimate for the unforced multidecadal variability is shown in Fig. 4.

The results indicate that during the periods 1910–1940 and 1970–2000 a warming of about 0.2 K can be attributed to internal variability. The magnitude of the long-term internal variability is in reasonable agreement with the findings of DelSole et al. (2011) who found a significant component of unforced multi-decadal variability in the recent acceleration of global warming, with $\pm 0.08^\circ\text{C}$ per decade for a 30 yr trend. Wu et al. (2011) estimated that up to one third of the late twentieth century warming could have been a consequence of natural variability. The model error terms are shown in Fig. 4. In the NH and for the global OHC the error term is mainly short-term fluctuations, while for the air temperatures in the SH there is also a multidecadal signal indicating that the correlation between the variability in the two hemispheres is different in the data than in CanESM2. The model error term includes several factors such as lack of explicit representation of the energy balance for land and ocean areas in each hemisphere, and possible shortcomings in the temporal development of the RF, etc.

4.4 Hemispheric difference in feedbacks

Figure 2e shows the estimated ECS in the sensitivity test where we have allowed for hemispheric differences in the climate sensitivity parameter. The difference between the hemispheric ECS estimated from the data was minor (20%), and the posterior estimate for the ECS was very close the main analysis.

4.5 Comparisons with results from a similar approach

Huber and Knutti (2012) used a similar approach and similar data as us, but their PDF of ECS was remarkable different from ours with a posterior estimate of 3.6°C and a much wider 90% C.I from 1.7 to 6.5°C Since their approach (Huber, 2011) is seemingly very similar to ours, it is worthwhile to discuss potential reasons for the differences. We will focus on two details that may lead to larger uncertainties, which

A lower and more constrained estimate of climate sensitivity

R. B. Skeie et al.

Title Page

Abstract

Introduction

Conclusions

References

Tables

Figures

◀

▶

◀

▶

Back

Close

Full Screen / Esc

Printer-friendly Version

Interactive Discussion



A lower and more constrained estimate of climate sensitivity

R. B. Skeie et al.

Title Page

Abstract

Introduction

Conclusions

References

Tables

Figures



Back

Close

Full Screen / Esc

Printer-friendly Version

Interactive Discussion



means that the ECS will be more similar to its prior distribution. These differences are: (i) although they use basically the same data series as us, they use only *one* temperature series and *one* OHC series per analysis, and make a simple average of these separate analyses at the end. As we have argued for above, using multiple observational series for the same quantity reduces the influence of the observational errors, especially for OHC, (ii) they don't use a simple climate model as our EBM, but instead they use a so called emulator. This emulator is based on a neural network model and is an approximation to a medium complex climate model. Therefore they have to introduce an extra error term to account for the approximation. For OHC, the approximation error is much larger than other error components (Fig. 4.2b in Huber, 2011). We believe that the effect of this is that the OHC data are considerably down-weighted compared to the temperature data, resulting in a high uncertainty in their ECS estimate.

5 Summary and conclusions

In this study, detailed RF time series for all well-established forcing mechanisms and observed OHC (0–700 m) and near-surface temperature change to year 2010 are combined in a Bayesian framework using a simple EBM and a stochastic model. The heavy tail often seen in PDFs of the ECS (Hegerl et al., 2007; Knutti and Hegerl, 2008; Huber and Knutti, 2012) is substantially reduced. The posterior mean estimate of the ECS is 1.8°C , outside of the likely range given in IPCC AR4 (Meehl et al., 2007), and probability of values larger than 4.5°C is only 1.4%. The majority of previous studies have not included temperature and OHC data over the last decade. Here we have used observational data including 2010, and we have shown that the combination of using multiple data series for surface temperatures and OHC and the additional 10 yr of data since year 2000, especially the OHC data, improve the constraint of the ECS. Using data only up to year 2000 and using one OHC data set as in previous studies, gave a significantly wider posterior distribution with a 90% C.I. of 1.1 to 14.5°C , with a heavy tail

of ice sheets. Also, the ECS estimates do not include biogeochemical-feedbacks for the LLGHGs which possibly can have affected historic concentrations and can have a large contribution for future climate change (Arneth et al., 2010).

Appendix A

Model description

We use a Bayesian approach where the RF time series and observations of ocean heat content (OHC) and near-surface temperature change are linked by a deterministic energy balance model (EBM) and a stochastic model to estimate the EBM parameters from the observational data. One of the model parameters is the equilibrium climate sensitivity (ECS).

In a Bayesian approach, parameters are assigned prior uncertainties, accounting for uncertainties in the knowledge of the parameter values. By combining this prior knowledge with observational data, the parameter values of a computer model can be constrained (Kennedy and O'Hagan, 2001). The Bayesian theorem is as follows:

$$P(\theta|\text{data}) \propto P(\theta) \cdot P(\text{data}|\theta)$$

where $P(\theta|\text{data})$, the posterior distribution of the parameters (θ) given the observational data, is proportional to the prior distribution of the parameters $P(\theta)$ multiplied by the likelihood of the data $P(\text{data}|\theta)$. Knowledge of the parameters can be gained by the observational data. It is important that the observational data used to constrain the parameters have not been used when the prior distributions of the parameters are decided.

The parameter of interest in this paper is the climate sensitivity, one out of several parameters in the EBM (see Table A1 below and Aldrin et al., 2012). The EBM is a deterministic model which calculates hemispheric mean temperature and ocean heat content with RF time series as input, and we combine the EBM with a stochastic model

A lower and more constrained estimate of climate sensitivity

R. B. Skeie et al.

Title Page

Abstract

Introduction

Conclusions

References

Tables

Figures

◀

▶

◀

▶

Back

Close

Full Screen / Esc

Printer-friendly Version

Interactive Discussion



to do inference. We here (in contrast to in the main text) describe the model by two equations, one for the underlying physical process and one for the data.

The process model:

$$\mathbf{g}_t = \mathbf{m}_t(\mathbf{x}_{1750:t}, \text{ECS}, \boldsymbol{\theta}) + \boldsymbol{\beta}_1 e_t + \mathbf{n}_t^{\text{liv}} + \mathbf{n}_t^{\text{m}}$$

5 and the data model:

$$\mathbf{y}_t = \mathbf{A}\mathbf{g}_t + \boldsymbol{\beta}_0 + \mathbf{n}_t^{\text{o}},$$

where \mathbf{g}_t is the true state of the world in year t (hemispheric temperature and ocean heat content), and $\mathbf{m}_t(\mathbf{x}_{1750:t}, \text{ECS}, \boldsymbol{\theta})$ is the EBM with RF time series as input $\mathbf{x}_{1750:t}$ and the climate sensitivity (ECS) as a parameter in addition to other parameters ($\boldsymbol{\theta}$).

10 The simple energy balance model is of reduced complexity and does not capture internal variability in the climate system such as the short-term El Niño-Southern Oscillation (ENSO) and more long-term oscillations. The ENSO effect is accounted for in the stochastic model using an index e_t and a vector of regression coefficients ($\boldsymbol{\beta}_1$), while long term internal variability is represented by the term $\mathbf{n}_t^{\text{liv}}$. For the model to represent
15 the true state of the world an error term \mathbf{n}_t^{m} is needed. The model error term includes limitations of the model system. The true state of the world is also represented in the data model by the observational data \mathbf{y}_t (hemispheric temperature and ocean heat content) and the observational error, \mathbf{n}_t^{o} . The matrix \mathbf{A} consists of 0s and 1s and is used for copying hemispheric temperatures and ocean heat content ground truth so
20 that the model output is compared with its corresponding observations. $\boldsymbol{\beta}_0$ is a vector of intercepts and is included because the measurements and output of the computer model are given relative to the mean of the different reference periods. The model errors are modelled as a vector autoregressive process of order one (VAR(1) process), while the observational errors are modelled as a scaled VAR(1) process, where the scaling factor is given by a vector of standard errors.

25 The long-term internal variability term $\mathbf{n}_t^{\text{liv}}$ is modelled as a vector autoregressive process of order three (VAR(3) process), i.e. $\mathbf{n}_t^{\text{liv}} = \boldsymbol{\phi}_1^{\text{liv}} \mathbf{n}_{t-1}^{\text{liv}} + \boldsymbol{\phi}_2^{\text{liv}} \mathbf{n}_{t-2}^{\text{liv}} + \boldsymbol{\phi}_3^{\text{liv}} \mathbf{n}_{t-3}^{\text{liv}} + \boldsymbol{\varepsilon}_t^{\text{liv}}$ and

A lower and more constrained estimate of climate sensitivity

R. B. Skeie et al.

Title Page

Abstract

Introduction

Conclusions

References

Tables

Figures



Back

Close

Full Screen / Esc

Printer-friendly Version

Interactive Discussion



A lower and more constrained estimate of climate sensitivity

R. B. Skeie et al.

Title Page

Abstract

Introduction

Conclusions

References

Tables

Figures

◀

▶

◀

▶

Back

Close

Full Screen / Esc

Printer-friendly Version

Interactive Discussion



$\text{Var}(\boldsymbol{\varepsilon}_t^{\text{liv}}) = \boldsymbol{\Sigma}^{\text{liv}} = \text{diag}(\boldsymbol{\sigma}^{\text{liv}})\mathbf{C}^{\text{liv}}\text{diag}(\boldsymbol{\sigma}^{\text{liv}})$, where the $\boldsymbol{\phi}$ -s are matrices with coefficients and where $\boldsymbol{\sigma}^{\text{liv}}$ and \mathbf{C}^{liv} are the standard deviations and correlation matrix of the covariance matrix, respectively. For estimating the parameters of this process, we use results for the Canadian CanESM2 in the CMIP5 experiment (Yang and Saenko, 2012) with simulations over 900 yr with zero RF. First we subtract a linear trend from the each of the temperature and OHC series to account for drift. Then we apply a 10 yr running mean to each of the three resulting time series (two for temperature, one for OHC). Furthermore, we estimate a VAR(3) process from these data, such that for instance the temperature at the Northern Hemisphere depends on the values of itself and the two other quantities the three preceding years. We include this VAR(3) process as an extra term ($\mathbf{n}_t^{\text{liv}}$) in our model, with all parameter values, except the standard deviations $\boldsymbol{\sigma}^{\text{liv}}$ of the errors $\boldsymbol{\varepsilon}_t^{\text{liv}}$, kept fixed (see Table A2). However, this is only an estimate of the internal variability. The magnitude may differ between different AOGCMs and Huber and Knutti (2012) claim that models underestimate internal variability with a factor of three. Therefore, we treat the standard deviations in the VAR(3) process as unknown parameters that we estimate, whereas the correlation structure is kept fixed. Note that in the model presented previously in Aldrin et al. (2012), we did not include the term $\mathbf{n}_t^{\text{liv}}$ in the process model. In that model long-term internal variability was accounted for by the model error term \mathbf{n}_t^{m} .

For applying a Bayesian approach, prior distributions of the model parameters and input data must be given. The input data, the RF time series for all well-established mechanisms, are estimated in this paper and given prior uncertainties based on ranges of published estimates and subjective assessments. The priors of ECS and $\boldsymbol{\theta} = (\theta^{\text{VHD}}, \theta^{\text{P}}, \theta^{\text{UV}}, \theta^{\text{ASHE}}, \theta^{\text{OIHE}}, \theta^{\text{M}})$ are given in Table A1, while all remaining parameters of the stochastic model, except the standard deviations in the VAR(3) process for long-term internal variability, are given vague priors. The reasoning behind the choice of priors of ECS and $\boldsymbol{\theta}$ is given in Supplement of Aldrin et al. (2012). The standard deviations in the VAR(3) process is modelled as $\boldsymbol{\sigma}^{\text{liv}} = \boldsymbol{\beta}_2 \boldsymbol{\sigma}_{\text{GCM}}^{\text{liv}}$, where $\boldsymbol{\sigma}_{\text{GCM}}^{\text{liv}}$ is the

standard deviations obtained when estimating the VAR(3) process from the CanESM2 data, and β_2 is a diagonal matrix where each diagonal element of β_2 is uniformly distributed between 1/5 and 5.

The EBM used in this study is the hemispheric version of the energy-balance climate/upwelling-diffusion ocean model described in Schlesinger et al. (1992) and its global version in Schlesinger and Jiang (1990). This model is a part of the CICERO SCM (Fuglestad and Berntsen, 1999) and has been used in several studies (e.g. Fuglestad et al., 2003; Rive et al., 2007; Skeie et al., 2009). The model has been shown to reproduce GCM model results from idealized experiments with a gradually changing forcing when the model parameters are calibrated (Olivie and Stuber, 2010). In the model the atmosphere is represented by a single layer and the ocean is subdivided into 40 vertical layers where the uppermost ocean layer is the mixed layer. Horizontally the model is divided into a northern and a Southern Hemisphere part, with a separate energy-balance calculation for each hemisphere. The hemispheric difference in land/ocean fraction is taken into account by scaling the efficiency of heat uptake by the ocean. This allows for more rapid response to forcings in the Northern Hemisphere. Each ocean box is divided into a polar and a non-polar region. In the polar region heat is transported from the mixed layer into the deep ocean representing deep water formation. In the non-polar region heat is transported downwards by processes treated as diffusion and advected upwards by slow upwelling. The representation of the ocean mixing is very simplified and does not include entrainment of downwelling water at intermediate depths as some other simple climate models do (e.g. MAGICC6 described in Meinshausen et al., 2011). As a consequence of this in the sensitivity test with observed deep ocean OHC (Fig. 2d) we treat all ocean below 700 m as one compartment.

The process model is updated by observed temperature change and ocean heat content y_t , taking into account uncertainties in the observational data, using a Markov Chain Monte Carlo (MCMC) algorithm. Posterior distributions of the climate sensitivity and other parameters are obtained. The statistical method is described in more detail

A lower and more constrained estimate of climate sensitivity

R. B. Skeie et al.

Title Page

Abstract

Introduction

Conclusions

References

Tables

Figures

◀

▶

◀

▶

Back

Close

Full Screen / Esc

Printer-friendly Version

Interactive Discussion



in Aldrin et al. (2012). Table A3 gives the MCMC parameter estimates for the main analysis, and three other key analyses. The estimates of standard deviations of the terms for ENSO, long-term internal variability and model errors are given in Table A4, while standard deviations of observational errors are given in Table A5.

Note that in the sensitivity test with two ECSs, one for the Northern Hemisphere (ECS_{NH}) and one for the Southern Hemisphere (ECS_{SH}), the prior for ECS is as in the main analysis, $\frac{ECS_{NH}+ECS_{SH}}{2} = ECS$, and $\log\left(\frac{ECS_{NH}}{ECS_{SH}}\right) \sim \text{Uniform}(-\log(1.5), \log(1.5))$. In the sensitivity test with two mixed layer depths, one for the Northern Hemisphere (θ_{NH}^M) and one for the Southern Hemisphere (θ_{SH}^M), the priors for θ_{NH}^M and θ_{SH}^M are set equal to the prior for θ^M in the main analysis.

Appendix B

Temperature and ocean heat content data

The temperature and ocean heat content data used in the analyses are shown in Figs. B1 and B2. The reported standard errors for the data in Fig. B1 are shown in Fig. B3, while posterior estimates of the standard deviations are shown in Fig. B4. Note that the posterior estimates of the standard deviations of the observational errors in Fig. B4 differ from those reported from the data providers (Fig. B3). Note especially that the posterior standard deviations for the three OHC series are much more equal than the reported ones, and that the posterior standard deviations for the Levitus series are roughly the double of the reported ones.

A lower and more constrained estimate of climate sensitivity

R. B. Skeie et al.

Title Page

Abstract

Introduction

Conclusions

References

Tables

Figures

◀

▶

◀

▶

Back

Close

Full Screen / Esc

Printer-friendly Version

Interactive Discussion



Natural forcing mechanisms

The natural forcing mechanisms included are stratospheric aerosols formed as a result of oxidation of sulfur dioxide emitted by explosive volcanic eruptions and changes in solar irradiance. The constructions of the natural radiative forcing time series used are described below.

C1 Solar variability

The time series for solar forcing is based on total solar irradiance (TSI) reconstruction of Wang et al. (2005) and the 11 yr cycle variation of Lean (2000). The change in TSI is multiplied by 0.25 to account for geometry, by 0.7 to account for the planetary albedo and by 0.78 according to Gray et al. (2009) accounting for changes in TSI at wavelengths where ozone absorbs strongly. The time series are extended from 2008 to 2010 using The Physikalisch-Meteorologisches Observatorium Davos (PMOD) composite (Frohlich and Lean, 2004). The RF over the full amplitude of the last solar cycle was 0.14 W m^{-2} . The uncertainty range for solar RF relative to pre-industrial times based on estimates from published studies given in IPCC AR4 (Forster et al., 2007) was skewed, ranging from 0.06 W m^{-2} to 0.3 W m^{-2} . The upper limit was based on TSI reconstructions using information from sun-like stars, which are called into question by Hall and Lockwood (2004). Recent estimates of changes in TSI (Delaygue and Bard, 2011; Krivova et al., 2007; Steinhilber et al., 2009; Tapping et al., 2007; Wang et al., 2005) are significantly lower than estimates using sun like stars (e.g. Lean, 2000). We use the relative uncertainty range $\pm 50\%$ spanning the relative uncertainty range in both Krivova et al. (2007) and Steinhilber et al. (2009), which are the same as the lower limit in IPCC AR4 (Forster et al., 2007).

A lower and more constrained estimate of climate sensitivity

R. B. Skeie et al.

Title Page

Abstract

Introduction

Conclusions

References

Tables

Figures

◀

▶

◀

▶

Back

Close

Full Screen / Esc

Printer-friendly Version

Interactive Discussion



C2 Explosive volcanic activity

We use three different time series for RF due to volcanoes and assign them an equal prior belief. The first time series are based on Gao et al. (2008). They presented stratospheric loading of aerosols for the past 1500 yr by using 54 ice core records from both the Arctic and Antarctica. We have followed the suggestions in Gao et al. (2008) and converted the aerosol loading to optical thickness for the years 1750 to 1980. Due to lack of coverage in the ice core data for the recent years we have replaced the data from Gao et al. (2008) after 1980 by the stratospheric aerosol optical thickness time series from Sato et al. (1993) based on satellite retrievals. The conversion factor between optical thickness and forcing used are -20 W m^{-2} (Wigley et al., 2005). The second time series for radiative forcing are the optical thickness data based on ice core records from Crowley et al. (2003) multiplied by the same conversion factor as above. The third volcanic radiative forcing time series used are from Ammann et al. (2003). The radiative forcing time series used are annual hemispheric means. We have extended all data sets using the updated values from Sato et al. (1993) for the period 2001 to 2010 (<http://data.giss.nasa.gov/modelforce/strataer/>, downloaded August 2011).

The reason for using three different estimates for RF from explosive volcanoes is to account for the uncertainty in the fluctuating pattern over time. For uncertainties in magnitude of the forcing we assume the quite conservative factor of 2. Smaller uncertainty intervals have been indicated in Gao et al. (2008) and in Sato et al. (1993).

Appendix D

Prior and posterior distributions for RF time series

The prior for each of the RF mechanisms is constructed by first constructing an expected or best guess time series for each hemisphere. These expectation curves are taken from the results in Skeie et al. (2011a). Then the uncertainties around the

ESDD

4, 785–852, 2013

A lower and more constrained estimate of climate sensitivity

R. B. Skeie et al.

Title Page

Abstract

Introduction

Conclusions

References

Tables

Figures

◀

▶

◀

▶

Back

Close

Full Screen / Esc

Printer-friendly Version

Interactive Discussion



A lower and more constrained estimate of climate sensitivity

R. B. Skeie et al.

Title Page

Abstract

Introduction

Conclusions

References

Tables

Figures

◀

▶

◀

▶

Back

Close

Full Screen / Esc

Printer-friendly Version

Interactive Discussion



expectation curves are constructed by adding or multiplying each number in the expectation by an error term, which gives a pair of NH and SH time series. The error terms are either the same for all time points and both hemispheres, or they are proportional to the number of years since 1750 times the expected value in 2010.

Four kinds of priors are assumed for the different RF mechanisms (Table 1): (1) normal distribution where the uncertainty/standard deviation is proportional to the expected value. (2) Normal distribution where the uncertainty/standard deviation is proportional to time. (3) Lognormal distribution where the uncertainty/standard deviation is proportional to the expected value. (4) Uniform distribution where the uncertainty/standard deviation is proportional to the values of a time series.

The uncertainty range for the RF mechanisms are based on Skeie et al. (2011a). If the 90 % confidence interval for the RF mechanisms include zero, there are no restrictions on the sign of the forcing, and a distribution where the uncertainty is proportional to time is chosen. The uncertainty in 1750 is zero. If the sign of the RF mechanisms is restricted, uncertainty proportional to expected value is chosen. If the given 90 % confidence interval is skewed, a lognormal distribution is chosen. A lognormal distribution is also chosen for forcing mechanisms with a symmetric 90 % confidence interval and a probability greater than 0.005 of RF with wrong sign. Otherwise, if the probability is less than 0.005, a normal distribution is chosen. For the lognormal distribution, the upper and lower quantile are dependent and will not exactly match the given 90 % confidence interval.

D1 Direct aerosol effect

The direct aerosol effect is the sum of five components: sulfate (SO_4), black carbon (BC) from fossil fuel and biofuel combustion (FFBF), organic matter (OM) (organic carbon from FFBF and secondary organic aerosols), biomass burning aerosols (BB) and nitrate aerosols (Nit).

For a given year we want the following statement A to be true: “The sum of the expected value for the aerosol components is equal to the expected value for total direct

aerosol effect.” Due to nonlinearities the sum of the individual aerosol direct effects is not identical to the total direct aerosol effect (Skeie et al., 2011a). For each year we find a constant a which is such that when we multiply each of the expected values for BC FFBF (SO_4 , OM, BB, Nit) with $1 + a(1 - a)$, the statement A is true. The values of the a 's are between -0.0177 and 0.0141 .

For 2010 we also want the following statement B to be true: “In year 2010 the sum of the variances for SO_4 , BC FFBF, OM, BB and Nit is equal to the variance for total direct aerosol effect”. We find a constant b which is such that when we multiply the standard deviations for SO_4 , BC FFBF, OM, BB and Nit, the statement B is true. We will also multiply the standard deviations before 2010 with a constant b . In 2000–2010: b is 0.603, before 1950: b is 1.00, 1950–2000: b decreases linearly from 1.0 to 0.603.

In Fig. 1 in the paper we show posterior RF time series and PDFs for RF in 2010 for the main analysis. Here (Fig. D1) we show the same results, but for the Northern and Southern Hemisphere separately.

Appendix E

Sensitivity tests

Here we describe some sensitivity tests performed with a somewhat simpler model setup using only one OHC dataset (from Levitus et al., 2009). Results are shown in Fig. E1.

There is no uncertainty in the RF time development (i.e. the temporal form of the curve) for each component or mechanism. We make sensitivity tests (Test 1 and Test 2) to see how changes in the prior assumptions for the time development of RF affect our result. In sensitivity Test 3 we test the sensitivity of our results to the role of uncertain data before 1900 (update with data only between 1900 and 2010 to exclude the uncertain early period including the 1883 Krakatoa volcanic eruption), while in sensitivity

A lower and more constrained estimate of climate sensitivity

R. B. Skeie et al.

Title Page

Abstract

Introduction

Conclusions

References

Tables

Figures

◀

▶

◀

▶

Back

Close

Full Screen / Esc

Printer-friendly Version

Interactive Discussion



Test 4 we test how the OHC data for the years 2001 to 2010 affect the ECS estimate by excluding OHC data from 2001 to 2010.

E1 Test 1: Change the BC direct aerosol effect in the latter part of the simulation period

5 Skeie et al. (2011b) calculated RF time series for Black Carbon (BC) from fossil fuel and biofuel (FFBF) sources using emission data from Bond et al. (2007). This emission scenario has a more rapid decrease in emissions in Europe and North America and a less rapid increase in emissions in Eastern Asia in the latter part of 20th century compared to the emission inventory (Lamarque et al., 2010) which are used for
10 constructing the RF time series for the main analysis.

As a sensitivity test we replace the RF time series for BC FFBF in the main analysis with data from Skeie et al. (2011b). This RF time series has a less rapid increase in the latter half of the 20th century compared to the RF time series used in the main analysis. The time series in Skeie et al. (2011b) ended in 2000, so the increase from 1990 to
15 2000 is extrapolated further to 2010. The change in the BC FFBF RF time series will also influence the semi-direct effect. The total direct aerosol effect is assumed to be the sum of all aerosol components in this sensitivity test.

In this sensitivity test the prior mean for the direct aerosol effect strengthens between 2000 and 2010 by -0.04 W m^{-2} compared to the main analysis where the direct aerosol effects weakened between 2000 and 2010 by 0.03 W m^{-2} . The altering of the temporal
20 structure of the prior RF had only very minor effects on the estimated ECS (Fig. E1d vs. E1b).

E2 Test 2: Change the BC direct aerosol effect in the first part of the simulation period

25 There are large uncertainties in the historical emission of BC (Bond et al., 2007). We modify the RF time series for BC FFBF (from the main analysis) from pre-industrial

A lower and more constrained estimate of climate sensitivity

R. B. Skeie et al.

Title Page

Abstract

Introduction

Conclusions

References

Tables

Figures



Back

Close

Full Screen / Esc

Printer-friendly Version

Interactive Discussion



times and up to 1960 to see if changes in the RF pattern early in the period affect the estimated ECS. There are indication of a too large BC concentration around 1850 and a too low concentration in early 20th century (Figs. 11 and 12 in Skeie et al., 2011b). As a sensitivity test we modify the time series of BC FFBF to have a more rapid increase in the end of the 19th century. Between 1750 and 1850 the RF time series is multiplied by 0.2 and between 1910 and 1940 multiplied by 1.3. We have linearly interpolated the multiplication factors for the years in between. After 1960 we use the same RF time series as in the main analysis, i.e. a multiplication factor of 1. As in Test 1, the change in the BC FFBF RF time series will also influence the semi-direct effect and the total direct aerosol effect.

The altering of the temporal structure of the prior RF had only very minor effects on the estimated ECS (Fig. E1e vs. E1b).

E3 Test 3: Updating the model with data between 1900 and 2010

Due to the large uncertainties in both the historical RF and observed temperature change we made another test where the model is only updated with data between 1900 and 2010 excluding the uncertain early period including the 1883 Krakatoa volcanic eruption. This sensitivity test slightly shift the ECS to larger values, increasing the posterior mean value by 0.3 °C to 2.2 °C and a 90 % C.I of 1.4 to 3.3 °C, but values larger than 4.5 °C are still basically excluded (Fig. E1f vs. E1b). The probability of ECS greater than 4.5 °C is 0.005.

E4 Test 4: The role of ocean heat content – excluding OHC data for the years 2001 to 2010

To test how the OHC data for the years 2000 to 2010 affect the ECS estimate, a sensitivity test is performed where the OHC data from 2000 to 2010 is excluded, i.e. OHC data between 2001 and 2010 are not used to update the model. The resulting PDF for the ECS (Fig. E1g) is significantly wider than in the corresponding full analysis

A lower and more constrained estimate of climate sensitivity

R. B. Skeie et al.

Title Page

Abstract

Introduction

Conclusions

References

Tables

Figures



Back

Close

Full Screen / Esc

Printer-friendly Version

Interactive Discussion



(Fig. E1b) and only slightly narrower than when only data up to year 2000 are used to estimate the ECS (Fig. E1c). The posterior mean for the ECS is 3.5°C and the probability of ECS being larger than 4.5°C is 0.17, so the estimated ECS is significantly constrained using the OHC data after year 2000.

5 E5 An additional sensitivity test with two mixed layer depths

We have performed an additional sensitivity test where we included two instead of one mixed layer depths. More precisely, we included one mixed layer depth for the Northern Hemisphere and one for the Southern Hemisphere. Note that in this sensitivity test long-term internal variability is included explicitly in the model and three OHC series are used, i.e. the sensitivity test is as the main analysis except for the inclusion of two mixed layer depths. The results are shown in Fig. E2. We observe that the inclusion of two mixed layer depths instead of one had only minor effects on the estimated ECS.

Appendix F

15 Pairs plots of samples from the posterior distribution

See Figs. F1 and F2.

Acknowledgements. This research was supported by the Norwegian Research Council under the projects “Constraining total feedback of the climate system by observations and models” (184840) and “An integrated Earth system approach to explore natural variability and climate sensitivity” (207711).

A lower and more constrained estimate of climate sensitivity

R. B. Skeie et al.

Title Page

Abstract

Introduction

Conclusions

References

Tables

Figures



Back

Close

Full Screen / Esc

Printer-friendly Version

Interactive Discussion



References

- Aldrin, M., Holden, M., Guttorp, P., Skeie, R. B., Myhre, G., and Berntsen, T. K.: Bayesian estimation of climate sensitivity based on a simple climate model fitted to observations of hemispheric temperatures and global ocean heat content, *Environmetrics*, 23, 253–271, 2012.
- 5 Allen, M. R. and Frame, D. J.: call off the quest, *Science*, 318, 582–583, 2007.
- Allen, M. R., Stott, P. A., Mitchell, J. F. B., Schnur, R., and Delworth, T. L.: Quantifying the uncertainty in forecasts of anthropogenic climate change, *Nature*, 407, 617–620, 2000.
- Ammann, C. M., Meehl, G. A., Washington, W. M., and Zender, C. S.: A monthly and latitudinally varying volcanic forcing dataset in simulations of 20th century climate, *Geophys. Res. Lett.*, 10 30, 1657, doi:10.1029/2003GL016875, 2003.
- Andreae, M. O., Jones, C. D., and Cox, P. M.: Strong present-day aerosol cooling implies a hot future, *Nature*, 435, 1187–1190, 2005.
- Andrews, E., Sheridan, P. J., and Ogren, J. A.: Seasonal differences in the vertical profiles of aerosol optical properties over rural Oklahoma, *Atmos. Chem. Phys.*, 11, 10661–10676, 15 doi:10.5194/acp-11-10661-2011, 2011.
- Andronova, N. G. and Schlesinger, M. E.: Objective estimation of the probability density function for climate sensitivity, *J. Geophys. Res.-Atmos.*, 106, 22605–22611, 2001.
- Annan, J. D. and Hargreaves, J. C.: Using multiple observationally-based constraints to estimate climate sensitivity, *Geophys. Res. Lett.*, 33, L06704, doi:10.1029/2005GL025259, 20 2006.
- Annan, J. D. and Hargreaves, J. C.: On the generation and interpretation of probabilistic estimates of climate sensitivity, *Climatic Change*, 104, 423–436, 2011.
- Annan, J. D., Hargreaves, J. C., Ohgaito, R., Abe-Ouchi, A., and Emori, S.: Efficiently constraining climate sensitivity with ensembles of paleoclimate simulations, *SOLA*, 1, 181–184, 25 2005.
- Arneth, A., Harrison, S. P., Zaehle, S., Tsigaridis, K., Menon, S., Bartlein, P. J., Feichter, J., Korhola, A., Kulmala, M., O'Donnell, D., Schurgers, G., Sorvari, S., and Vesala, T.: Terrestrial biogeochemical feedbacks in the climate system, *Nat. Geosci.*, 3, 525–532, 2010.
- Arora, V. K., Boer, G., Friedlingstein, P., Eby, M., Jones, C., Christian, J., Bonan, G., Bopp, L., Brovkin, V., Cadule, P., Hajima, T., Ilyina, T., Lindsay, K., Tjiputra, J., and Wu, T.: The Effect of terrestrial photosynthesis down regulation on the twentieth-century carbon budget simulated with the CCCma Earth System Model, *J. Climate*, 22, 6066–6088, 2009.
- 30

ESDD

4, 785–852, 2013

A lower and more constrained estimate of climate sensitivity

R. B. Skeie et al.

Title Page

Abstract

Introduction

Conclusions

References

Tables

Figures

◀

▶

◀

▶

Back

Close

Full Screen / Esc

Printer-friendly Version

Interactive Discussion



A lower and more constrained estimate of climate sensitivity

R. B. Skeie et al.

Title Page

Abstract

Introduction

Conclusions

References

Tables

Figures

◀

▶

◀

▶

Back

Close

Full Screen / Esc

Printer-friendly Version

Interactive Discussion



- Bond, T. C., Bhardwaj, E., Dong, R., Jogani, R., Jung, S., Roden, C., Streets, D. G., and Trautmann, N. M.: Historical emissions of black and organic carbon aerosol from energy-related combustion, 1850–2000, *Global Biogeochem. Cy.*, 21, GB2018, doi:10.1029/2006GB002840, 2007.
- 5 Boucher, O. and Haywood, J.: On summing the components of radiative forcing of climate change, *Clim. Dynam.*, 18, 297–302, 2001.
- Brohan, P., Kennedy, J. J., Harris, I., Tett, S. F. B., and Jones, P. D.: Uncertainty estimates in regional and global observed temperature changes: a new data set from 1850, *J. Geophys. Res.-Atmos.*, 111, D12106, doi:10.1029/2005JD006548, 2006.
- 10 Church, J. A., White, N. J., Konikow, L. F., Domingues, C. M., Cogley, J. G., Rignot, E., Gregory, J. M., van den Broeke, M. R., Monaghan A. J., and Velicogna, I.: Revisiting the Earth's sea-level and energy budgets from 1961 to 2008, *Geophys. Res. Lett.*, 38, L18601, doi:10.1029/2011GL048794, 2011.
- Crowley, T. J., Baum, S. K., Kim, K. Y., Hegerl, G. C., and Hyde, W. T.: Modeling ocean heat content changes during the last millennium, *Geophys. Res. Lett.*, 30, 1932, doi:10.1029/2003GL017801, 2003.
- 15 Cubasch, U., Meehl, G. A., Boer, G. J., Stouffer, R. J., Dix, M., Noda, A., Senior, C. A., Raper, S., and Yap, K. S.: Projections of Future Climate Change, in: *Climate Change 2001: The Scientific Basis, Contribution of Working Group I to the Fourth Assessment Report of the Intergovernmental Panel on Climate Change*, edited by: Houghton, J. T., Ding, Y., Griggs, D. J., Noguer, M., van der Linden, P. J., Dai, X., Maskell, K., and Johnson, C. A., Cambridge University Press, 2001.
- Delaygue, G. and Bard, E.: An Antarctic view of Beryllium-10 and solar activity for the past millennium, *Clim. Dynam.*, 36, 2201–2218, 2011.
- 25 DelSole, T., Tippet, M. K., and Shukla, J.: A significant component of unforced multidecadal variability in the recent acceleration of global warming, *J. Climate*, 24, 909–926, 2011.
- Denman, K. L., Brasseur, G., Chidthaisong, A., Ciais, P., Cox, P. M., Dickinson, R. E., Didier Hauglustaine, D., Heinze, C., Holland, E., Jacob, D., Lohmann, U., Ramachandran, S., da Silva Dias, P. L., Wofsy, S. C., and Zhang, X.: Couplings between changes in the climate system and biogeochemistry, in: *Climate Change 2007: The Physical Science Basis. Contribution of Working Group I to the Fourth Assessment Report of the Intergovernmental Panel on Climate Change*, edited by: Solomon, S., Qin, D., Manning, M., Chen, Z., Marquis, M., Averyt, K. B., Tignor, M., and Miller, H. L., 2007.
- 30

A lower and more constrained estimate of climate sensitivity

R. B. Skeie et al.

Title Page

Abstract

Introduction

Conclusions

References

Tables

Figures

◀

▶

◀

▶

Back

Close

Full Screen / Esc

Printer-friendly Version

Interactive Discussion



Domingues, C. M., Church, J. A., White, N. J., Gleckler, P. J., Wijffels, S. E., Barker, P. M., and Dunn, J. R.: Improved estimates of upper-ocean warming and multi-decadal sea-level rise, *Nature*, 453, 1090–1094, 2008.

Easterling, D. R. and Wehner, M. F.: Is the climate warming or cooling?, *Geophys. Res. Lett.*, 36, L08706, doi:10.1029/2009GL037810, 2009.

Fiore, A. M., Dentener, F. J., Wild, O., Cuvelier, C., Schultz, M. G., Hess, P., Textor, C., Schulz, M., Doherty, R. M., Horowitz, L. W., MacKenzie, I. A., Sanderson, M. G., Shindell, D. T., Stevenson, D. S., Szopa, S., Van Dingenen, R., Zeng, G., Atherton, C., Bergmann, D., Bey, I., Carmichael, G., Collins, W. J., Duncan, B. N., Faluvegi, G., Folberth, G., Gauss, M., Gong, S., Hauglustaine, D., Holloway, T., Isaksen, I. S. A., Jacob, D. J., Jonson, J. E., Kaminski, J. W., Keating, T. J., Lupu, A., Marmer, E., Montanaro, V., Park, R. J., Pitari, G., Pringle, K. J., Pyle, J. A., Schroeder, S., Vivanco, M. G., Wind, P., Wojcik, G., Wu, S., and Zuber, A.: Multimodel estimates of intercontinental source-receptor relationships for ozone pollution, *J. Geophys. Res.-Atmos.*, 114, D04301, doi:10.1029/2008JD010816, 2009.

Forest, C. E., Stone, P. H., Sokolov, A. P., Allen, M. R., and Webster, M. D.: Quantifying uncertainties in climate system properties with the use of recent climate observations, *Science*, 295, 113–117, 2002.

Forest, C. E., Stone, P. H., and Sokolov, A. P.: Estimated PDFs of climate system properties including natural and anthropogenic forcings, *Geophys. Res. Lett.*, 33, L01705, doi:10.1029/2005GL023977, 2006.

Forest, C. E., Stone, P. H., and Sokolov, A. P.: Constraining climate model parameters from observed 20th century changes, *Tellus A*, 60, 911–920, 2008.

Forster, P., Ramaswamy, V., Artaxo, P., Bernsten, T., Betts, R., Fahey, D. W., Haywood, J., Lean, J., Lowe, D. C., Myhre, G., Nganga, J., Prinn, R., Raga, G., Schulz, M., and Van Dorland, R.: Changes in atmospheric constituents and in radiative forcing, in: *Climate Change 2007: The Physical Science Basis. Contribution of Working Group I to the Fourth Assessment Report of the Intergovernmental Panel on Climate Change*, edited by: Solomon, S., Qin, D., Manning, M., Chen, Z., Marquis, M., Averyt, K. B., Tignor, M., and Miller, H. L., Cambridge Univ. Press., 2007.

Frame, D. J., Booth, B. B. B., Kettleborough, J. A., Stainforth, D. A., Gregory, J. M., Collins, M., and Allen, M. R.: Constraining climate forecasts: the role of prior assumptions, *Geophys. Res. Lett.*, 32, 1–5, 2005.

A lower and more constrained estimate of climate sensitivity

R. B. Skeie et al.

Title Page

Abstract

Introduction

Conclusions

References

Tables

Figures

◀

▶

◀

▶

Back

Close

Full Screen / Esc

Printer-friendly Version

Interactive Discussion



- Frohlich, C. and Lean, J.: Solar radiative output and its variability: evidence and mechanisms, *Astron. Astrophys. Rev.*, 12, 273–320, 2004.
- Fuglestedt, J. S. and Berntsen, T.: A Simple Model for Scenario Studies of Changes in Global Climate: Version 1.0, CICERO working paper 1999:2, available at: <http://www.cicero.uio.no/media/187.pdf> (last access 6 August 2013), 1999.
- Fuglestedt, J. S., Berntsen, T. K., Godal, O., Sausen, R., Shine, K. P., and Skodvin, T.: Metrics of climate change: assessing radiative forcing and emission indices, *Climatic Change*, 58, 267–331, 2003.
- Gao, C. C., Robock, A., and Ammann, C.: Volcanic forcing of climate over the past 1500 years: an improved ice core-based index for climate models, *J. Geophys. Res.*, 113, D23111, doi:10.1029/2008JD010239, 2008.
- Gillett, N. P., Arora, V. K., Flato, G. M., Scinocca, J. F., and von Salzen, K.: Improved constraints on 21st-century warming derived using 160 years of temperature observations, *Geophys. Res. Lett.*, 39, L01704, doi:10.1029/2011GL050226, 2012.
- Gouretski, V. and Koltermann, K. P.: How much is the ocean really warming?, *Geophys. Res. Lett.*, 34, L01610, doi:10.1029/2006GL027834, 2007.
- Gray, L. J., Rumbold, S. T., and Shine, K. P.: Stratospheric temperature and radiative forcing response to 11-year solar cycle changes in irradiance and ozone, *J. Atmos. Sci.*, 66, 2402–2417, 2009.
- Gregory, J. M. and Forster, P. M.: Transient climate response estimated from radiative forcing and observed temperature change, *J. Geophys. Res.-Atmos.*, 113, D23105, doi:10.1029/2008JD010405, 2008.
- Gregory, J. M., Stouffer, R. J., Raper, S. C. B., Stott, P. A., and Rayner, N. A.: An observationally based estimate of the climate sensitivity, *J. Climate*, 15, 3117–3121, 2002.
- Hall, J. C. and Lockwood, G. W.: The chromospheric activity and variability of cycling and flat activity solar-analog stars, *Astrophys. J.*, 614, 942–946, 2004.
- Hannart, A., Dufresne, J. L., and Naveau, P.: Why climate sensitivity may not be so unpredictable, *Geophys. Res. Lett.*, 36, L16707, doi:10.1029/2009GL039640, 2009.
- Hansen, J. E. and Sato, M.: Paleoclimate implications for human-made climate change, in: *Climate Change: Inferences from Paleoclimate and Regional Aspects*, edited by: Berger, A., Mesinger, F., and Šijački, D., Springer, 21–48, 2012.
- Hansen, J., Russell, G., Laxis, A., Fung, I., Rind, D., and Stone, P.: Climate response-times – dependence on climate sensitivity and ocean mixing, *Science*, 229, 857–859, 1985.

A lower and more constrained estimate of climate sensitivity

R. B. Skeie et al.

Title Page

Abstract

Introduction

Conclusions

References

Tables

Figures

◀

▶

◀

▶

Back

Close

Full Screen / Esc

Printer-friendly Version

Interactive Discussion



Hansen, J., Sato, M., Ruedy, R., Nazarenko, L., Lacis, A., Schmidt, G. A., Russell, G., Aleinov, I., Bauer, M., Bauer, S., Bell, N., Cairns, B., Canuto, V., Chandler, M., Cheng, Y., Del Genio, A., Faluvegi, G., Fleming, E., Friend, A., Hall, T., Jackman, C., Kelley, M., Kiang, N., Koch, D., Lean, J., Lerner, J., Lo, K., Menon, S., Miller, R., Minnis, P., Novakov, T., Oinas, V., Perlwitz, J., Perlwitz, J., Rind, D., Romanou, A., Shindell, D., Stone, P., Sun, S., Tausnev, N., Thresher, D., Wielicki, B., Wong, T., Yao, M., and Zhang, S.: Efficacy of climate forcings, *J. Geophys. Res.-Atmos.*, 110, D18104, doi:10.1029/2005JD005776, 2005.

Hansen, J., Sato, M., Ruedy, R., Lo, K., Lea, D. W., and Medina-Elizade, M.: Global temperature change, *P. Natl. Acad. Sci. USA*, 103, 14288–14293, 2006.

Hansen, J., Ruedy, R., Sato, M., and Lo, K.: Global surface temperature change, *Rev. Geophys.*, 48, Rg4004, doi:10.1029/2010RG000345, 2010.

Hansen, J., Sato, M., Kharecha, P., and von Schuckmann, K.: Earth's energy imbalance and implications, *Atmos. Chem. Phys.*, 11, 13421–13449, doi:10.5194/acp-11-13421-2011, 2011.

Hegerl, G. C., Crowley, T. J., Hyde, W. T., and Frame, D. J.: Climate sensitivity constrained by temperature reconstructions over the past seven centuries, *Nature*, 440, 1029–1032, 2006.

Hegerl, G. C., Zwiers, F. C., Braconnot, P., Gillett, N. P., Luo, Y., Marengo Orsini, J. A., Nicholls, N., Penner, J. P., and Stott, P. A.: Understanding and attributing climate change, in: *Climate Change 2007: The Physical Science Basis. Contribution of Working Group I to the Fourth Assessment Report of the Intergovernmental Panel on Climate Change*, edited by: Solomon, S., Qin, D., Manning, M., Chen, Z., Marquis, M., Averyt, K. B., Tignor, M., and Miller, H. L., Cambridge Univ. Press., 2007.

Huber, M. B.: The Earth's Energy Balance and its Changes: Implications for Past and Future Temperature Change, Ph.D. thesis, ETH, Zurich, Switzerland, doi:10.3929/ethz-a-006689560, 2011.

Huber, M. and Knutti, R.: Anthropogenic and natural warming inferred from changes in Earth's energy balance, *Nat. Geosci.*, 5, 31–36, doi:10.1038/NGEO1327, 2012.

Isaksen, I. S. A., Granier, C., Myhre, G., Berntsen, T. K., Dalsoren, S. B., Gauss, M., Klimont, Z., Benestad, R., Bousquet, P., Collins, W., Cox, T., Eyring, V., Fowler, D., Fuzzi, S., Jockel, P., Laj, P., Lohmann, U., Maione, M., Monks, P., Prevo, A. S. H., Raes, F., Richter, A., Rognerud, B., Schulz, M., Shindell, D., Stevenson, D. S., Storelvmo, T., Wang, W.-C., van Weele, M., Wild, M., and Wuebbles, D.: Atmospheric composition change: climate-chemistry interactions, *Atmos. Environ.*, 43, 5138–5192, 2009.

A lower and more constrained estimate of climate sensitivity

R. B. Skeie et al.

Title Page

Abstract

Introduction

Conclusions

References

Tables

Figures

◀

▶

◀

▶

Back

Close

Full Screen / Esc

Printer-friendly Version

Interactive Discussion



- Ishii, M. and Kimoto, M.: Reevaluation of historical ocean heat content variations with time-varying XBT and MBT depth bias corrections, *J. Oceanogr.*, 65, 287–299, 2009.
- Joshi, M., Shine, K., Ponater, M., Stuber, N., Sausen, R., and Li, L.: A comparison of climate response to different radiative forcings in three general circulation models: towards an improved metric of climate change, *Clim. Dynam.*, 20, 843–854, 2003.
- Kaufmann, R. K., Kauppi, H., Mann, M. L., and Stock, J. H.: Reconciling anthropogenic climate change with observed temperature 1998–2008, *P. Natl. Acad. Sci. USA*, 108, 11790–11793, 2011.
- Kennedy, M. C. and O’Hagan, A.: Bayesian calibration of computer models. *J. Roy. Stat. Soc. B*, 63, 425–450, 2001.
- Kerr, R. A.: A North Atlantic climate pacemaker for the centuries, *Science*, 288, 1984–1986, 2000.
- Knight, J. R.: The Atlantic multidecadal oscillation inferred from the forced climate response in coupled general circulation models, *J. Climate*, 22, 1610–1625, 2009.
- Knutti, R. and Hegerl, G. C.: The equilibrium sensitivity of the Earth’s temperature to radiation changes, *Nat. Geosci.*, 1, 735–743, 2008.
- Knutti, R. and Tomassini, L.: Constraints on the transient climate response from observed global temperature and ocean heat uptake, *Geophys. Res. Lett.*, 35, L09701, doi:10.1029/2008GL034932, 2008.
- Knutti, R., Stocker, T. F., Joos, F., and Plattner, G.-K.: Constraints on radiative forcing and future climate change from observations and climate model ensembles, *Nature*, 416, 719–723, 2002.
- Kohler, P., Bintanja, R., Fischer, H., Joos, F., Knutti, R., Lohmann, G., and Masson-Delmotte, V.: What caused Earth’s temperature variations during the last 800,000 years? Data-based evidence on radiative forcing and constraints on climate sensitivity, *Quaternary Sci. Rev.*, 29, 129–145, 2010.
- Kouketsu, S., Doi, T., Kawano, T., Masuda, S., Sugiura, N., Sasaki, Y., Toyoda, T., Igarashi, H., Kawai, Y., Katsumata, K., Uchida, H., Fukasawa, M., and Awaji, T.: Deep ocean heat content changes estimated from observation and reanalysis product and their influence on sea level change, *J. Geophys. Res.-Oceans*, 116, C03012, doi:10.1029/2010JC006464, 2011.
- Krivova, N. A., Balmaceda, L., and Solanki, S. K.: Reconstruction of solar total irradiance since 1700 from the surface magnetic flux, *Astron. Astrophys.*, 467, 335–346, 2007.

A lower and more constrained estimate of climate sensitivity

R. B. Skeie et al.

Title Page

Abstract

Introduction

Conclusions

References

Tables

Figures

◀

▶

◀

▶

Back

Close

Full Screen / Esc

Printer-friendly Version

Interactive Discussion



- Lamarque, J.-F., Bond, T. C., Eyring, V., Granier, C., Heil, A., Klimont, Z., Lee, D., Lioussé, C., Mieville, A., Owen, B., Schultz, M. G., Shindell, D., Smith, S. J., Stehfest, E., Van Aardenne, J., Cooper, O. R., Kainuma, M., Mahowald, N., McConnell, J. R., Naik, V., Riahi, K., and van Vuuren, D. P.: Historical (1850–2000) gridded anthropogenic and biomass burning emissions of reactive gases and aerosols: methodology and application, *Atmos. Chem. Phys.*, 10, 7017–7039, doi:10.5194/acp-10-7017-2010, 2010.
- Lean, J.: Evolution of the sun's spectral irradiance since the Maunder Minimum, *Geophys. Res. Lett.*, 27, 2425–2428, 2000.
- Levitus, S., Antonov, J. I., Boyer, T. P., Locarnini, R. A., Garcia, H. E., and Mishonov, A. V.: Global ocean heat content 1955–2008 in light of recently revealed instrumentation problems, *Geophys. Res. Lett.*, 36, L07608, doi:10.1029/2008GL037155, 2009.
- Levitus, S., Antonov, J. I., Boyer, T. P., Baranova, O. K., Garcia, H. E., Locarnini, R. A., Mishonov, A. V., Reagan, J. R., Seidov, D., Yarosh, E. S., and Zweng, M.: World ocean heat content and thermocline sea level change (0–2000,m), 1955–2010, *Geophys. Res. Lett.*, 39, L10603, doi:10.1029/2012GL051106, 2012.
- Lewis, N.: An objective Bayesian, improved approach for applying optimal fingerprint techniques to estimate climate sensitivity, *J. Climate*, online first, doi:10.1175/JCLI-D-12-00473.1, 2013.
- Libardoni, C. E. and Forest, A. G.: Sensitivity of distributions of climate system properties to the surface temperature dataset, *Geophys. Res. Lett.*, 38, L22705, doi:10.1029/2011GL049431, 2011.
- Loeb, G. L., Lyman, J. M., Johnson, G. C., Allan, R. P., Doelling, D. R., Wong, T., Soden, B. J., and Stephens, G. L.: Observed changes in top-of-the-atmosphere radiation and upper-ocean heating consistent within uncertainty, *Nat. Geosci.*, 5, 110–113, 2012.
- Lohmann, U., Rotstayn, L., Storelvmo, T., Jones, A., Menon, S., Quaas, J., Ekman, A. M. L., Koch, D., and Ruedy, R.: Total aerosol effect: radiative forcing or radiative flux perturbation?, *Atmos. Chem. Phys.*, 10, 3235–3246, doi:10.5194/acp-10-3235-2010, 2010.
- Lu, Z., Zhang, Q., and Streets, D. G.: Sulfur dioxide and primary carbonaceous aerosol emissions in China and India, 1996–2010, *Atmos. Chem. Phys.*, 11, 9839–9864, doi:10.5194/acp-11-9839-2011, 2011.
- Lyman, J. M., Good, S. A., Gouretski, V. V., Ishii, M., Johnson, G. C., Palmer, M. D., Smith, D. M., and Willis, J. K.: Robust warming of the global upper ocean, *Nature*, 465, 334–337, 2010.

A lower and more constrained estimate of climate sensitivity

R. B. Skeie et al.

Title Page

Abstract

Introduction

Conclusions

References

Tables

Figures

◀

▶

◀

▶

Back

Close

Full Screen / Esc

Printer-friendly Version

Interactive Discussion



- Meehl, G. A., Stocker, T. F., Collins, W. D., Friedlingstein, P., Gaye, A. T., Gregory, J. M., Kitoh, A., Knutti, R., Murphy, J. M., Noda, A., Raper, S. C. B., Watterson, I. G., Weaver, A. J., and Zhao, Z.-C.: Global climate projections, in: *Climate Change 2007: The Physical Science Basis. Contribution of Working Group I to the Fourth Assessment Report of the Intergovernmental Panel on Climate Change*, edited by: Solomon, S., Qin, D., Manning, M., Chen, Z., Marquis, M., Averyt, K. B., Tignor, M., and Miller, H. L., 2007.
- Meehl, G. A., Arblaster, J. M., Fasullo, J. T., Hu, A., and Trenberth, K. E.: Model-based evidence of deep-ocean heat uptake during surface-temperature hiatus periods, *Nature Climate Change*, 1, 360–364, 2011.
- Meinshausen, M., Meinshausen, N., Hare, W., Raper, S. C. B., Frieler, K., Knutti, R., Frame, D. J., and Allen, M. R.: Greenhouse-gas emission targets for limiting global warming to 2 °C, *Nature*, 458, 1158–1162, 2009.
- Meinshausen, M., Wigley, T. M. L., and Raper, S. C. B.: Emulating atmosphere-ocean and carbon cycle models with a simpler model, *MAGICC6 – Part 2: Applications, Atmos. Chem. Phys.*, 11, 1457–1471, doi:10.5194/acp-11-1457-2011, 2011.
- Morice, C. P., Kennedy, J. J., Rayner, N. A., and Jones, P. D.: Quantifying uncertainties in global and regional temperature change using an ensemble of observational estimates: the HadCRUT4 data set, *J. Geophys. Res.-Atmos.*, 117, D08101, doi:10.1029/2011JD017187, 2012.
- Murphy, D. M., Solomon, S., Portmann, R. W., Rosenlof, K. H., Forster, P. M., and Wong, T.: An observationally based energy balance for the Earth since 1950, *J. Geophys. Res.-Atmos.*, 114, D17107, doi:10.1029/2009JD012105, 2009.
- Murphy, J. M.: Transient response of the Hadley Centre coupled ocean-atmosphere model to increasing carbon dioxide, Part I: control climate and flux adjustment, *J. Climate*, 8, 36–56, 1995.
- Murphy, J. M., Sexton, D. M. H., Barnett, D. N., Jones, G. S., Webb, M. J., and Collins, M.: Quantification of modelling uncertainties in a large ensemble of climate change simulations, *Nature*, 430, 768–772, 2004.
- Myhre, G.: Consistency between satellite-derived and modeled estimates of the direct aerosol effect, *Science*, 325, 187–190, 2009.
- Olivie, D. and Stuber, N.: Emulating AOGCM results using simple climate models, *Clim. Dynam.*, 35, 1257–1287, 2010.

A lower and more constrained estimate of climate sensitivity

R. B. Skeie et al.

Title Page

Abstract

Introduction

Conclusions

References

Tables

Figures



Back

Close

Full Screen / Esc

Printer-friendly Version

Interactive Discussion



Olson, R., Sriver, R., Goes, M., Urban, N. M., Damon Matthews, H., Haran, M., and Keller, K.: A climate sensitivity estimate using Bayesian fusion of instrumental observations and an Earth System model, *J. Geophys. Res.-Atmos.*, 117, D04103, doi:10.1029/2011JD016620, 2012.

5 Ottera, O. H., Bentsen, M., Drange, H., and Suo, L.: External forcing as a metronome for Atlantic multidecadal variability, *Nat. Geosci.*, 3, 688–694, 2010.

Otto, A., Otto, F. E. L., Boucher, O., Church, J., Hegerl, G., Forster, P. M., Nathan, P., Gillett, N. P., Gregory, J., Johnson, G. C., Knutti, R., Lewis, N., Lohmann, U., Marotzke, J., Myhre, G., Shindell, D., Stevens, B., and Allen, M. P.: Energy budget constraints on climate response, *Nat. Geosci.*, 6, 415–416, doi:10.1038/ngeo1836, 2013.

10 Padilla, L. E., Vallis, G. K., and Rowley, C. W.: Probabilistic estimates of transient climate sensitivity subject to uncertainty in forcing and natural variability, *J. Climate*, 24, 5521–5537, 2011.

15 Palmer, M., Antonov, J., Barker, P., Bindoff, N., Boyer, T., Carson, M., Domingues, C., Gille, S., Gleckler, P., Good, S., Gouretski, V., Guinehut, S., Haines, K., Harrison, D. E., Ishii, M., Johnson, G., Levitus, S., Lozier, S., Lyman, J., Meijers, A., von Shuckmann, K., Smith, D., Wijffels, S., and Willis, J.: Future Observations for Monitoring Global Ocean Heat Content, in: *Proceedings of the “OceanObs’ 09: Sustained Ocean Observations and Information for Society” Conference (Vol. 2)*, Venice, Italy, 21–25 September 2009, edited by: Hall, J., Harrison, D. E., and Stammer, D., ESA Publication WPP-306, 2010.

20 Palmer, M. D., McNeall, D. J., and Dunstone, N. J.: Importance of the deep ocean for estimating decadal changes in Earth’s radiation balance, *Geophys. Res. Lett.*, 38, L13707, doi:10.1029/2011GL047835, 2011.

25 Penner, J. E., Chen, Y., Wang, M., and Liu, X.: Possible influence of anthropogenic aerosols on cirrus clouds and anthropogenic forcing, *Atmos. Chem. Phys.*, 9, 879–896, doi:10.5194/acp-9-879-2009, 2009.

Piani, C., Frame, D. J., Stainforth, D. A., and Allen, M. R.: Constraints on climate change from a multi-thousand member ensemble of simulations, *Geophys. Res. Lett.*, 32, L23825, doi:10.1029/2005GL024452, 2005.

30 Purkey, S. G. and Johnson, G. C.: Warming of global abyssal and deep Southern Ocean waters between the 1990s and 2000s: contributions to global heat and sea level rise budgets, *J. Climate*, 23, 6336–6351, 2010.

A lower and more constrained estimate of climate sensitivity

R. B. Skeie et al.

Title Page

Abstract

Introduction

Conclusions

References

Tables

Figures

◀

▶

◀

▶

Back

Close

Full Screen / Esc

Printer-friendly Version

Interactive Discussion



- Raper, S. C. B., Gregory, J. M., and Osborn, T. J.: Use of an upwelling-diffusion energy balance climate model to simulate and diagnose A/OGCM results, *Clim. Dynam.*, 17, 601–613, 2001.
- Ring, M. J., Lindner, D., Cross, E. F., and Schlesinger, M. E.: Causes of the global warming observed since the 19th century, *Atmos. Clim. Sci.*, 2, 401–415, 2012.
- 5 Rive, N., Torvanger, A., Berntsen, T., and Kallbekken, S.: To what extent can a long-term temperature target guide near-term climate change commitments?, *Climatic Change*, 82, 373–391, 2007.
- Roe, G. H. and Armour, K. C.: How sensitive is climate sensitivity?, *Geophys. Res. Lett.*, 38, L14708, doi:10.1029/2011GL047913, 2011.
- 10 Roe, G. H. and Baker, M. B.: Why is climate sensitivity so unpredictable?, *Science*, 318, 629–632, 2007.
- Royer, D. L., Berner, R. A., and Park, J.: Climate sensitivity constrained by CO₂ concentrations over the past 420 million years, *Nature*, 446, 530–532, 2007.
- Sato, M., Hansen, J. E., McCormick, M. P., and Pollack, J. B.: Stratospheric aerosol optical depths, 1850–1990, *J. Geophys. Res.-Atmos.*, 98, 22987–22994, 1993.
- 15 Schlesinger, M. E. and Jiang, X. J.: Simple-model representation of atmosphere-ocean GCMs and estimation of the time scale of CO₂-induced climate change, *J. Climate*, 3, 1297–1315, 1990.
- Schlesinger, M. E., Jiang, X., and Charlson, R. J.: Implication of Anthropogenic Atmospheric Sulphate for the Sensitivity of the Climate System. *Climate Change and Energy Policy*, in: *Proceedings of the International Conference on Global Climate Change: Its Mitigation Through Improved Production and Use of Energy*, edited by: Rosen, L. and Glasser, R., American Institute of Physics, 75–108, 1992.
- 20 Schmittner, A., Urban, N. M., Shakun, J. D., Mahowald, N. M., Clark, P. U., Bartlein, P. J., Mix, A. C., and Rosell-Melé, A.: Climate sensitivity estimated from temperature reconstructions of the last glacial maximum, *Science*, 334, 1385–1388, doi:10.1126/science.1203513, 2011.
- Schneider von Deimling, T., Held, H., Ganopolski, A., and Rahmstorf, S.: Climate sensitivity estimated from ensemble simulations of glacial climate, *Clim. Dynam.*, 27, 149–163, 2006.
- 25 Skeie, R. B., Fuglestad, J., Berntsen, T., Lund, M. T., Myhre, G., and Rypdal, K.: Global temperature change from the transport sectors: historical development and future scenarios, *Atmos. Environ.*, 43, 6260–6270, 2009.
- 30

A lower and more constrained estimate of climate sensitivity

R. B. Skeie et al.

Title Page

Abstract

Introduction

Conclusions

References

Tables

Figures

◀

▶

◀

▶

Back

Close

Full Screen / Esc

Printer-friendly Version

Interactive Discussion



- Skeie, R. B., Berntsen, T. K., Myhre, G., Tanaka, K., Kvalevåg, M. M., and Hoyle, C. R.: Anthropogenic radiative forcing time series from pre-industrial times until 2010, *Atmos. Chem. Phys.*, 11, 11827–11857, doi:10.5194/acp-11-11827-2011, 2011a.
- Skeie, R. B., Berntsen, T., Myhre, G., Pedersen, C. A., Ström, J., Gerland, S., and Ogren, J. A.: Black carbon in the atmosphere and snow, from pre-industrial times until present, *Atmos. Chem. Phys.*, 11, 6809–6836, doi:10.5194/acp-11-6809-2011, 2011b.
- Smith, T. M. and Reynolds, R. W.: A global merged land-air-sea surface temperature reconstruction based on historical observations (1880–1997), *J. Climate*, 18, 2021–2036, 2005.
- Smith, T. M., Reynolds, R. W., Peterson, T. C., and Lawrimore, J.: Improvements to NOAA's historical merged land-ocean surface temperature analysis (1880–2006), *J. Climate*, 21, 2283–2296, 2008.
- Sokolov, A. P., Forest, C. E., and Stone, P. H.: Comparing oceanic heat uptake in AOGCM transient climate change experiments, *J. Climate*, 16, 1573–1582, 2003.
- Solomon, S., Rosenlof, K. H., Portmann, R. W., Daniel, J. S., Davis, S. M., Sanford, T. J., and Plattner, G.-K.: Contributions of stratospheric water vapor to decadal changes in the rate of global warming, *Science*, 327, 1219–1223, 2010.
- Solomon, S., Daniel, J. S., Neely, R. R., Vernier, J.-P., Dutton, E. G., and Thomason, L. W.: The persistently variable “background” stratospheric aerosol layer and global climate change, *Science*, 333, 866–870, 2011.
- Stainforth, D. A., Aina, T., Christensen, C., Collins, M., Faull, N., Frame, D. J., Kettleborough, J. A., Knight, S., Martin, A., Murphy, J. M., Piani, C., Sexton, D., Smith, L. A., Spicer, R. A., Thorpe, A. J., and Allen, M. R.: Uncertainty in predictions of the climate response to rising levels of greenhouse gases, *Nature*, 433, 403–406, 2005.
- Steinhilber, F., Beer, J., and Frohlich, C.: Total solar irradiance during the Holocene, *Geophys. Res. Lett.*, 36, L19704, doi:10.1029/2009GL040142, 2009.
- Stott, C. E. and Forest, P. A.: Ensemble climate predictions using climate models and observational constraints, *Philos. T. R. Soc. A*, 365, 2029–2052, doi:10.1098/rsta.2007.2075, 2007.
- Stott, P. A., Mitchell, J. F. B., Allen, M. R., Delworth, T. L., Gregory, J. M., Meehl, G. A., and Santer, B. D.: Observational constraints on past attributable warming and predictions of future global warming, *J. Climate*, 19, 3055–3069, 2006.
- Tanaka, K., Raddatz, T., O'Neill, B. C., and Reick, C. H.: Insufficient forcing uncertainty underestimates the risk of high climate sensitivity, *Geophys. Res. Lett.*, 36, L16709, doi:10.1029/2009GL039642, 2009.

A lower and more constrained estimate of climate sensitivity

R. B. Skeie et al.

Title Page

Abstract

Introduction

Conclusions

References

Tables

Figures

◀

▶

◀

▶

Back

Close

Full Screen / Esc

Printer-friendly Version

Interactive Discussion



Tapping, K. F., Boteler, D., Charbonneau, P., Crouch, A., Manson, A., and Paquette, H.: Solar magnetic activity and total irradiance since the maunder minimum, *Sol. Phys.*, 246, 309–326, 2007.

Thompson, D. W. J., Kennedy, J. J., Wallace, J. M., and Jones, P. D.: A large discontinuity in the mid-twentieth century in observed global-mean surface temperature, *Nature*, 453, 646–649, 2008.

Thompson, D. W. J., Wallace, J. M., Kennedy, J. J., and Jones, P. D.: An abrupt drop in Northern Hemisphere sea surface temperature around 1970, *Nature*, 467, 444–447, 2010.

Tomassini, L., Reichert, P., Knutti, R., Stocker, T. F., and Borsuk, M. E.: Robust Bayesian uncertainty analysis of climate system properties using Markov chain Monte Carlo methods, *J. Climate*, 20, 1239–1254, 2007.

Trenberth, K. E. and Fasullo, J. T.: Tracking Earth's energy, *Science*, 328, 316–317, 2010.

Trenberth, K. E., Caron, J. M., Stepaniak, D. P., and Worley, S.: Evolution of El Niño–Southern Oscillation and global atmospheric surface temperatures, *J. Geophys. Res.-Atmos.*, 107, 4065, doi:10.1029/2000JD000298, 2002.

Trenberth, K., Jones, P. D., Ambenje, P., Bojariu, R., Easterling, D., Klein Tank, A., Parker, D., Rahimzadeh, F., Renwick, J. A., Rusticucci, M., Soden, B., and Zhai, P.: Observations: surface and atmospheric climate change, in: *Climate Change 2007: The Physical Science Basis. Contribution of Working Group I to the Fourth Assessment Report of the Intergovernmental Panel on Climate*, edited by: Solomon, S., Qin, D., Manning, M., Chen, Z., Marquis, M., Averyt, K. B., Tignor, M., and Miller, H. L., Cambridge Univ. Press., 2007.

UNFCCC: Report of the Conference of the Parties on Its Fifteenth Session, held in Copenhagen from 7 to 19 December 2009 (FCCC/CP/2009/11/Add.1, United Nations, 2010), available at: <http://unfccc.int/resource/docs/2009/cop15/eng/11a01.pdf> (last access: January 2013), 2009.

UNFCCC: Report of the Conference of the Parties on Its Sixteenth Session, held in Cancun from 29 November to 10 December 2010 (FCCC/CP/2010/7/Add.1, United Nations, 2011), available at: <http://unfccc.int/resource/docs/2010/cop16/eng/07a01.pdf> (last access: January 2013), 2010.

Urban, N. M. and Keller, K.: Complementary observational constraints on climate sensitivity, *Geophys. Res. Lett.*, 36, L04708, doi:10.1029/2008GL036457, 2009.

Vernier, J. P., Thomason, L. W., Pommereau, J.-P., Bourassa, A., Pelon, J., Garnier, A., Hauchecorne, A., Blanot, L., Trepte, C., Degenstein, D., and Vargas, F.: Major influence of

A lower and more constrained estimate of climate sensitivity

R. B. Skeie et al.

Title Page

Abstract

Introduction

Conclusions

References

Tables

Figures

◀

▶

◀

▶

Back

Close

Full Screen / Esc

Printer-friendly Version

Interactive Discussion



tropical volcanic eruptions on the stratospheric aerosol layer during the last decade, *Geophys. Res. Lett.*, 38, L12807, doi:10.1029/2011GL047563, 2011.

von Schuckmann, K. and Le Traon, P.-Y.: How well can we derive Global Ocean Indicators from Argo data?, *Ocean Sci.*, 7, 783–791, doi:10.5194/os-7-783-2011, 2011.

5 Wang, Y. M., Lean, J. L., and Sheeley, N. R.: Modeling the sun's magnetic field and irradiance since 1713, *Astrophys. J.*, 625, 522–538, 2005.

Wigley, T. M. L. and Schlesinger, M. E.: Analytical solution for the effect of increasing CO₂ on global mean temperature, *Nature*, 315, 649–652, 1985.

10 Wigley, T. M. L., Ammann, C. M., Santer, B. D., and Raper, S. C. B.: Effect of climate sensitivity on the response to volcanic forcing, *J. Geophys. Res.*, 110, D09107, doi:10.1029/2004JD005557, 2005.

Wild, M., Trüssel, B., Ohmura, A., Long, C. N., König-Langlo, G., Dutton, E. G., and Tsvetkov, A.: Global dimming and brightening: an update beyond 2000, *J. Geophys. Res.-Atmos.*, 114, D00D13, doi:10.1029/2008JD011382, 2009.

15 Wu, Z., Huang, N., Wallace, J., Smoliak, B., and Chen, X.: On the time-varying trend in global-mean surface temperature, *Clim. Dynam.*, 37, 759–773, 2011.

Yang, D. and Saenko, O. A.: Ocean heat transport and its projected change in CanESM2, *J. Climate*, 25, 8148–8163, 2012.

20 Zhang, Q., Streets, D. G., Carmichael, G. R., He, K. B., Huo, H., Kannari, A., Klimont, Z., Park, I. S., Reddy, S., Fu, J. S., Chen, D., Duan, L., Lei, Y., Wang, L. T., and Yao, Z. L.: Asian emissions in 2006 for the NASA INTEX-B mission, *Atmos. Chem. Phys.*, 9, 5131–5153, doi:10.5194/acp-9-5131-2009, 2009.

A lower and more constrained estimate of climate sensitivity

R. B. Skeie et al.

Table 1. The RF mechanisms included with information on the prior distribution assumed and the prior mean value and the 90 % confidence interval in year 2010. The RF values are relative to 1750.

RF mechanisms	Prior distribution	Prior mean (Wm^{-2}) in 2010			90 % confidence interval (Wm^{-2}) in 2010		
Long lived greenhouse gases (LLGHGs)	Normal	2.83	2.54	3.11			
Tropospheric O_3	Normal	0.44	0.31	0.57			
Stratospheric O_3	Lognormal	-0.23	-0.41	-0.11			
Stratospheric H_2O from CH_4	Lognormal	0.07	0.04	0.13			
<i>Direct aerosol effects:</i>							
Sulfate	Normal	-0.63	-0.83	-0.44			
BC fossil fuel and biofuel (FFBF)	Lognormal	0.50	0.30	0.75			
OC FFBF + secondary organic aerosols	Lognormal	-0.22	-0.35	-0.13			
Biomass burning aerosols	Normal, proportional to time	-0.07	-0.14	0.00			
Nitrate	Lognormal	-0.05	-0.07	-0.03			
Total direct aerosol effect	Sum of aerosol RFs above	-0.48	-0.80	-0.13			
<i>Indirect aerosol effects:</i>							
Cloud albedo effect	Normal	-0.83	-1.35	-0.34			
Cloud lifetime effect	Lognormal	-0.35	-1.34	-0.01			
Semi-direct aerosol effect	Uniform, proportional to BC FFBF	$(-0.25, +0.50)^a$					
<i>Surface albedo changes:</i>							
Snow albedo effect	Lognormal	0.02	0.00	0.06			
Land use change	Lognormal	-0.10	-0.21	-0.04			
<i>Natural RF:</i>							
Volcanoes ^b	Lognormal	-0.06	-0.11	-0.03			
Solar irradiance ^c	Normal, proportional to time	0.08	0.04	0.13			

^a See also Sect. 2.3.

^b The RF is the average 2001–2010.

^c The RF is the average over the last 11 yr compared to average of 11 yr around 1750.

Title Page

Abstract

Introduction

Conclusions

References

Tables

Figures

◀

▶

◀

▶

Back

Close

Full Screen / Esc

Printer-friendly Version

Interactive Discussion



A lower and more constrained estimate of climate sensitivity

R. B. Skeie et al.

Table A1. Priors of ECS and the other model parameters θ .

Name		Unit	Range
Mixed layer depth	θ^M	m	25–125
Vertical heat diffusivity	θ^{VHD}	$\text{cm}^2 \text{s}^{-1}$	0.06–0.8*
Polar parameter	θ^P	–	0.161–0.0569
Vertical velocity, upwelling rate	θ^{UV}	m yr^{-1}	0.55–2.55
Air–sea heat exchange parameter	θ^{ASHE}	$\text{W (m}^2 \text{K)}^{-1}$	5–25
Oceanic inter hemispheric heat exchange coefficient	θ^{OIHE}	$\text{W (m}^2 \text{K)}^{-1}$	0–7
Climate sensitivity	ECS	K	0–20

* $\theta^{VHD} = H\theta^{UV}$, where H is the scale depth. Range of H : 400–1000 m. H is uniform, θ^{VHD} is not.

Title Page

Abstract

Introduction

Conclusions

References

Tables

Figures

◀

▶

◀

▶

Back

Close

Full Screen / Esc

Printer-friendly Version

Interactive Discussion



A lower and more constrained estimate of climate sensitivity

R. B. Skeie et al.

Title Page

Abstract

Introduction

Conclusions

References

Tables

Figures

◀

▶

◀

▶

Back

Close

Full Screen / Esc

Printer-friendly Version

Interactive Discussion



Table A2. Parameter estimates (posterior means) for the VAR(3) process in the main analysis.

		NH	SH	OHC
ϕ_1^{liv}	NH	1.428	0.004	-0.858
	SH	-0.127	1.058	1.173
	OHC	0.125	0.163	2.216
ϕ_2^{liv}	NH	-0.466	-0.063	1.136
	SH	0.178	0.057	1.642
	OHC	-0.209	-0.280	-1.534
ϕ_3^{liv}	NH	-0.015	0.066	-0.398
	SH	-0.053	-0.182	-0.565
	OHC	0.086	0.118	0.316
$\sigma_{\text{GCM}}^{\text{liv}}$		0.016	0.017	0.040
\mathbf{C}^{liv}	NH	1.000	0.438	0.146
	SH	0.438	1.000	0.209
	OHC	0.146	0.209	1.000

Table A3. Parameter estimates with 95 % C.I. In the table $\boldsymbol{\varphi}^m$ and $\boldsymbol{\varphi}^o$ are the diagonal coefficient matrices of the VAR(1) processes for the model and observational errors, respectively, and $\boldsymbol{\sigma}^m/\mathbf{C}^m$ and $\boldsymbol{\sigma}^o/\mathbf{C}^o$ are the standard deviations/correlation matrices of the covariance matrix $\boldsymbol{\Sigma}^m$ and $\boldsymbol{\Sigma}^o$ of the error terms of the VAR(1) processes for the model and observational errors, respectively, i.e. $\boldsymbol{\Sigma}^m = \text{diag}(\boldsymbol{\sigma}^m)\mathbf{C}^m\text{diag}(\boldsymbol{\sigma}^m)$ and $\boldsymbol{\Sigma}^o = \text{diag}(\boldsymbol{\sigma}^o)\mathbf{C}^o\text{diag}(\boldsymbol{\sigma}^o)$. For each analysis there are at least 140 million iterations after burn-in in the MCMC estimation algorithm.

Parameter	Main analysis	Main analysis, but with data up to 2000–3 OHC	Main analysis, but with data up to 2000–1 OHC	Main analysis, but without internal variability
θ				
θ^{VHD}	0.28 (0.1,0.59)	0.34 (0.11,0.68)	0.4 (0.13,0.72)	0.24 (0.1,0.49)
θ^p	0.37 (0.17,0.56)	0.37 (0.17,0.56)	0.37 (0.17,0.56)	0.37 (0.17,0.56)
θ^{LV}	1.37 (0.58,2.46)	1.55 (0.6,2.5)	1.72 (0.64,2.52)	1.25 (0.57,2.41)
θ^{ASHE}	13.53 (5.25,24.31)	13.2 (5.26,24.27)	12.81 (5.24,24.17)	13.63 (5.27,24.35)
θ^{OHE}	3.6 (0.25,6.84)	3.69 (0.26,6.83)	3.87 (0.4,6.84)	3.55 (0.23,6.83)
θ^m	59 (26,114)	59 (27,121)	60 (29,123)	56 (26,109)
β_0				
NH1	-0.01 (-0.03,0)	-0.02 (-0.03,0)	-0.02 (-0.04,0)	-0.01 (-0.03,0)
NH2	0.01 (-0.01,0.04)	0.01 (-0.02,0.03)	0.01 (-0.02,0.03)	0.01 (-0.01,0.04)
NH3	0.03 (0.01,0.04)	0.03 (0.01,0.04)	0.03 (0.01,0.04)	0.02 (0.01,0.04)
SH1	-0.03 (-0.06,-0.01)	-0.03 (-0.06,-0.01)	-0.03 (-0.06,0)	-0.03 (-0.06,-0.01)
SH2	-0.01 (-0.04,0.01)	-0.01 (-0.04,0.02)	-0.01 (-0.04,0.02)	-0.02 (-0.04,0.01)
SH3	-0.03 (-0.04,-0.02)	-0.03 (-0.04,-0.02)	-0.03 (-0.04,-0.02)	-0.03 (-0.05,-0.02)
OHC1	0.95 (0.39,1.53)	-0.29 (-0.79,0.22)	-0.67 (-1.04,-0.07)	0.96 (0.39,1.56)
OHC2	3.86 (1.96,6.15)	4.23 (1.69,7.7)		3.91 (1.87,6.27)
OHC3	-0.21 (-2.49,2.57)	0.18 (-1.98,2.98)		0 (-2.64,2.94)
β_1				
NH	-5e-04 (-8e-04,-3e-04)	-5e-04 (-8e-04,-2e-04)	-5e-04 (-8e-04,-2e-04)	-5e-04 (-8e-04,-3e-04)
SH	-4e-04 (-6e-04,-2e-04)	-4e-04 (-7e-04,-2e-04)	-4e-04 (-7e-04,-2e-04)	-4e-04 (-6e-04,-2e-04)
β_2				
NH	1.53 (0.53,2.99)	1.57 (0.51,3.33)	1.58 (0.5,3.39)	1.53 (0.53,2.99)
SH	1.55 (0.53,3.07)	1.71 (0.59,3.58)	1.77 (0.59,3.69)	1.55 (0.53,3.07)
OHC	2.94 (1.27,4.74)	3.34 (1.56,4.87)	3.31 (1.51,4.87)	2.94 (1.27,4.74)
$\boldsymbol{\varphi}^m$				
NH	0.56 (0.27,0.84)	0.55 (0.26,0.83)	0.56 (0.28,0.83)	0.64 (0.45,0.83)
SH	0.71 (0.43,0.93)	0.7 (0.42,0.92)	0.73 (0.46,0.94)	0.74 (0.57,0.91)
OHC	0.46 (-0.19,0.95)	0.14 (-0.5,0.87)	-0.16 (-0.75,0.67)	0.61 (0.13,0.96)
$\boldsymbol{\varphi}^o$				
NH	0.6 (0.49,0.71)	0.61 (0.49,0.72)	0.61 (0.5,0.72)	0.6 (0.49,0.72)
SH	0.54 (0.42,0.65)	0.57 (0.45,0.7)	0.58 (0.46,0.7)	0.54 (0.42,0.66)
OHC	0.89 (0.78,0.97)	0.87 (0.75,0.96)	0.52 (0.04,0.9)	0.89 (0.79,0.97)
$\boldsymbol{\sigma}^m$				
NH	0.13 (0.11,0.15)	0.13 (0.12,0.15)	0.14 (0.12,0.15)	0.13 (0.12,0.15)
SH	0.11 (0.1,0.13)	0.12 (0.1,0.13)	0.12 (0.1,0.13)	0.11 (0.1,0.13)
OHC	0.62 (0.4,0.87)	0.67 (0.44,0.96)	0.67 (0.39,1.05)	0.67 (0.47,0.93)
\mathbf{C}^m				
NH-SH	0.19 (0.02,0.36)	0.2 (0.02,0.37)	0.2 (0.03,0.37)	0.21 (0.05,0.37)
NH-OHC	0.04 (-0.18,0.26)	0.03 (-0.2,0.26)	-0.01 (-0.24,0.23)	0.06 (-0.16,0.29)
SH-OHC	0.02 (-0.19,0.23)	0.01 (-0.21,0.23)	-0.01 (-0.23,0.22)	0.03 (-0.17,0.24)
$\boldsymbol{\sigma}^o$				
NH1	0.48 (0.34,0.66)	0.49 (0.34,0.67)	0.5 (0.35,0.69)	0.5 (0.36,0.69)
NH2	0.77 (0.58,0.99)	0.77 (0.58,0.99)	0.79 (0.59,1.02)	0.78 (0.59,1)
NH3	0.38 (0.26,0.54)	0.38 (0.26,0.54)	0.38 (0.26,0.55)	0.39 (0.27,0.55)
SH1	0.63 (0.5,0.79)	0.64 (0.5,0.81)	0.65 (0.51,0.82)	0.65 (0.51,0.8)
SH2	0.98 (0.78,1.19)	0.97 (0.77,1.2)	0.98 (0.78,1.21)	0.97 (0.78,1.2)
SH3	0.43 (0.28,0.65)	0.44 (0.28,0.67)	0.45 (0.29,0.67)	0.45 (0.29,0.67)
OHC1	1.59 (0.91,2.29)	1 (0.57,1.65)	0.85 (0.49,1.33)	1.67 (1.02,2.35)
OHC2	0.42 (0.31,0.57)	0.44 (0.33,0.57)		0.42 (0.31,0.56)
OHC3	0.65 (0.48,0.84)	0.6 (0.44,0.81)		0.66 (0.49,0.85)

A lower and more constrained estimate of climate sensitivity

R. B. Skeie et al.

Title Page

Abstract

Introduction

Conclusions

References

Tables

Figures

⏪

⏩

◀

▶

Back

Close

Full Screen / Esc

Printer-friendly Version

Interactive Discussion



A lower and more constrained estimate of climate sensitivity

R. B. Skeie et al.

Table A3. Continued.

Parameter	Main analysis	Main analysis, but with data up to 2000–3 OHC	Main analysis, but with data up to 2000–1 OHC	Main analysis, but without internal variability
φ^m				
NH	0.56 (0.27,0.84)	0.55 (0.26,0.83)	0.56 (0.28,0.83)	0.64 (0.45,0.83)
SH	0.71 (0.43,0.93)	0.7 (0.42,0.92)	0.73 (0.46,0.94)	0.74 (0.57,0.91)
OHC	0.46 (–0.19,0.95)	0.14 (–0.5,0.87)	–0.16 (–0.75,0.67)	0.61 (0.13,0.96)
φ^o				
NH	0.6 (0.49,0.71)	0.61 (0.49,0.72)	0.61 (0.5,0.72)	0.6 (0.49,0.72)
SH	0.54 (0.42,0.65)	0.57 (0.45,0.7)	0.58 (0.46,0.7)	0.54 (0.42,0.66)
OHC	0.89 (0.78,0.97)	0.87 (0.75,0.96)	0.52 (0.04,0.9)	0.89 (0.79,0.97)
σ^m				
NH	0.13 (0.11,0.15)	0.13 (0.12,0.15)	0.14 (0.12,0.15)	0.13 (0.12,0.15)
SH	0.11 (0.1,0.13)	0.12 (0.1,0.13)	0.12 (0.1,0.13)	0.11 (0.1,0.13)
OHC	0.62 (0.4,0.87)	0.67 (0.44,0.96)	0.67 (0.39,1.05)	0.67 (0.47,0.93)
σ^m				
NH-SH	0.19 (0.02,0.36)	0.2 (0.02,0.37)	0.2 (0.03,0.37)	0.21 (0.05,0.37)
NH-OHC	0.04 (–0.18,0.26)	0.03 (–0.2,0.26)	–0.01 (–0.24,0.23)	0.06 (–0.16,0.29)
SH-OHC	0.02 (–0.19,0.23)	0.01 (–0.21,0.23)	–0.01 (–0.23,0.22)	0.03 (–0.17,0.24)
σ^o				
NH1	0.48 (0.34,0.66)	0.49 (0.34,0.67)	0.5 (0.35,0.69)	0.5 (0.36,0.69)
NH2	0.77 (0.58,0.99)	0.77 (0.58,0.99)	0.79 (0.59,1.02)	0.78 (0.59,1)
NH3	0.38 (0.26,0.54)	0.38 (0.26,0.54)	0.38 (0.26,0.55)	0.39 (0.27,0.55)
SH1	0.63 (0.5,0.79)	0.64 (0.5,0.81)	0.65 (0.51,0.82)	0.65 (0.51,0.8)
SH2	0.96 (0.78,1.19)	0.97 (0.77,1.2)	0.97 (0.78,1.21)	0.97 (0.78,1.2)
SH3	0.43 (0.28,0.65)	0.44 (0.28,0.67)	0.45 (0.29,0.69)	0.45 (0.29,0.67)
OHC1	1.59 (0.91,2.29)	1 (0.57,1.65)	0.85 (0.49,1.33)	1.67 (1.02,2.35)
OHC2	0.42 (0.31,0.57)	0.44 (0.33,0.57)		0.42 (0.31,0.56)
OHC3	0.65 (0.48,0.84)	0.6 (0.44,0.81)		0.66 (0.49,0.85)
σ^o				
NH1-NH2	0.29 (–0.16,0.63)	0.32 (–0.12,0.65)	0.36 (–0.08,0.68)	0.31 (–0.12,0.64)
NH1-NH3	0.4 (–0.02,0.72)	0.4 (–0.04,0.73)	0.43 (–0.01,0.74)	0.45 (0.04,0.74)
NH1-SH1	0.2 (–0.23,0.57)	0.2 (–0.24,0.58)	0.19 (–0.24,0.57)	0.2 (–0.21,0.57)
NH1-SH2	–0.06 (–0.49,0.38)	–0.07 (–0.49,0.37)	–0.08 (–0.5,0.37)	–0.08 (–0.49,0.35)
NH1-SH3	0.1 (–0.39,0.54)	0.07 (–0.42,0.53)	0.06 (–0.43,0.53)	0.11 (–0.37,0.55)
NH1-OHC1	–0.22 (–0.65,0.28)	–0.24 (–0.66,0.27)	–0.17 (–0.65,0.39)	–0.22 (–0.64,0.27)
NH1-OHC2	0.06 (–0.36,0.46)	0.13 (–0.28,0.49)		0.05 (–0.36,0.45)
NH1-OHC3	–0.17 (–0.55,0.27)	–0.08 (–0.49,0.36)		–0.2 (–0.57,0.24)
NH2-NH3	0.49 (0.02,0.79)	0.51 (0.04,0.81)	0.55 (0.08,0.82)	0.51 (0.05,0.8)
NH2-SH1	0.1 (–0.23,0.42)	0.1 (–0.24,0.43)	0.11 (–0.24,0.43)	0.09 (–0.24,0.4)
NH2-SH2	0.09 (–0.26,0.42)	0.05 (–0.31,0.39)	0.04 (–0.31,0.38)	0.05 (–0.29,0.39)
NH2-SH3	–0.07 (–0.55,0.44)	–0.09 (–0.57,0.43)	–0.08 (–0.56,0.42)	–0.09 (–0.56,0.4)
NH2-OHC1	–0.06 (–0.45,0.34)	0.2 (–0.26,0.6)	0.24 (–0.28,0.68)	–0.07 (–0.44,0.32)
NH2-OHC2	0.1 (–0.21,0.41)	–0.03 (–0.34,0.28)		0.1 (–0.22,0.4)
NH2-OHC3	–0.02 (–0.34,0.31)	0 (–0.34,0.35)		–0.02 (–0.34,0.3)
NH3-SH1	0.21 (–0.25,0.61)	0.21 (–0.27,0.61)	0.21 (–0.28,0.61)	0.21 (–0.25,0.59)
NH3-SH2	0 (–0.54,0.53)	–0.07 (–0.6,0.5)	–0.07 (–0.6,0.5)	–0.05 (–0.57,0.49)
NH3-SH3	0.04 (–0.47,0.53)	0.01 (–0.51,0.52)	0.01 (–0.52,0.52)	0.03 (–0.47,0.51)
NH3-OHC1	–0.18 (–0.68,0.42)	0.06 (–0.5,0.6)	0.09 (–0.49,0.62)	–0.19 (–0.67,0.38)
NH3-OHC2	0.16 (–0.32,0.58)	–0.04 (–0.49,0.43)		0.16 (–0.32,0.57)
NH3-OHC3	0.08 (–0.4,0.53)	0.04 (–0.44,0.51)		0.05 (–0.41,0.5)
SH1-SH2	0.25 (–0.03,0.5)	0.23 (–0.07,0.48)	0.25 (–0.04,0.5)	0.26 (–0.02,0.5)
SH1-SH3	0.49 (0.09,0.76)	0.49 (0.09,0.76)	0.52 (0.13,0.78)	0.52 (0.14,0.76)
SH1-OHC1	–0.02 (–0.38,0.33)	0.14 (–0.29,0.52)	0.19 (–0.33,0.62)	–0.03 (–0.39,0.31)
SH1-OHC2	0.05 (–0.25,0.34)	–0.08 (–0.39,0.24)		0.05 (–0.25,0.34)
SH1-OHC3	0.13 (–0.21,0.45)	0.14 (–0.25,0.48)		0.13 (–0.21,0.44)
SH2-SH3	0.51 (–0.05,0.83)	0.53 (–0.02,0.84)	0.56 (0.04,0.85)	0.5 (–0.04,0.82)
SH2-OHC1	0.01 (–0.28,0.31)	0.31 (–0.05,0.64)	0.4 (–0.05,0.75)	–0.02 (–0.3,0.27)
SH2-OHC2	0.1 (–0.16,0.35)	–0.03 (–0.3,0.25)		0.09 (–0.17,0.34)
SH2-OHC3	0.03 (–0.25,0.31)	0.11 (–0.2,0.4)		0.02 (–0.27,0.29)
SH3-OHC1	–0.03 (–0.54,0.49)	0.13 (–0.41,0.61)	0.2 (–0.37,0.67)	–0.06 (–0.55,0.45)
SH3-OHC2	0.05 (–0.39,0.47)	–0.04 (–0.46,0.4)		0.05 (–0.38,0.46)
SH3-OHC3	0.06 (–0.41,0.51)	0.1 (–0.37,0.54)		0.05 (–0.41,0.49)
OHC1-OHC2	–0.59 (–0.8,–0.28)	–0.48 (–0.75,–0.09)		–0.57 (–0.79,–0.27)
OHC1-OHC3	0.22 (–0.27,0.57)	0.09 (–0.4,0.52)		0.26 (–0.19,0.59)
OHC2-OHC3	–0.02 (–0.37,0.34)	0.02 (–0.34,0.38)		–0.03 (–0.37,0.33)

Title Page

Abstract

Introduction

Conclusions

References

Tables

Figures



Back

Close

Full Screen / Esc

Printer-friendly Version

Interactive Discussion



A lower and more constrained estimate of climate sensitivity

R. B. Skeie et al.

Table A4. Estimates of standard deviations of $\beta_1 e_t$, n_t^{liv} , n_t^{m} and the sum of these three terms.

	$\beta_1 e_t$	n_t^{liv}	n_t^{m}	$\beta_1 e_t + n_t^{\text{liv}} + n_t^{\text{m}}$
NH	0.045	0.098	0.157	0.191
SH	0.038	0.086	0.159	0.185
(NH + SH)/2	0.041	0.075	0.122	0.149
OHC	0.000	2.853	0.697	2.933

Title Page

Abstract

Introduction

Conclusions

References

Tables

Figures

◀

▶

◀

▶

Back

Close

Full Screen / Esc

Printer-friendly Version

Interactive Discussion



A lower and more constrained estimate of climate sensitivity

R. B. Skeie et al.

Table A5. Estimates of standard deviations of n_t^o .

St.dev. n_t^o	In 1960	In 2000	Mean over observation period	Mean over 1991–2010
NH1	0.027	0.032	0.043	0.032
SH1	0.048	0.048	0.061	0.048
(NH1 + SH1)/2	0.030	0.031	0.040	0.032
NH2	0.034	0.052	0.072	0.050
SH2	0.054	0.053	0.083	0.053
(NH2 + SH2)/2	0.040	0.048	0.071	0.047
NH3	0.012	0.026	0.041	0.024
SH3	0.016	0.014	0.034	0.014
(NH3 + SH3)/2	0.010	0.015	0.027	0.014
OHC1	1.700	1.966	2.257	1.668
OHC2	5.624	1.686	3.349	1.320
OHC3	2.090	1.802	1.898	1.696

Title Page

Abstract

Introduction

Conclusions

References

Tables

Figures

◀

▶

◀

▶

Back

Close

Full Screen / Esc

Printer-friendly Version

Interactive Discussion



A lower and more constrained estimate of climate sensitivity

R. B. Skeie et al.

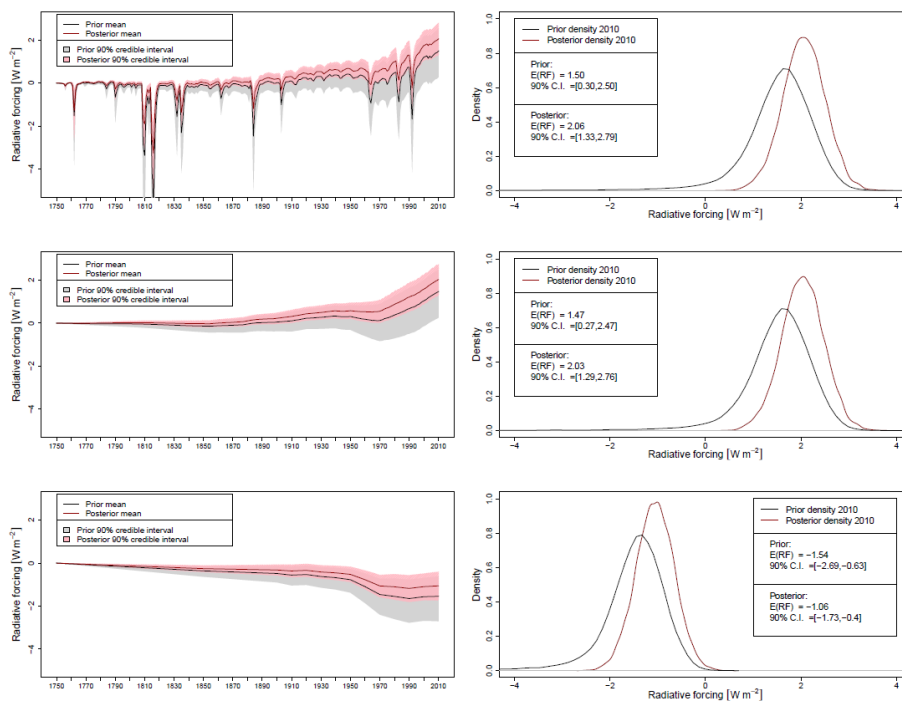


Fig. 1. Prior and posterior distribution of the RF time series and PDF of RF in 2010 for total RF (upper panel), anthropogenic RF (middle panel) and total aerosol effect (direct effect, cloud albedo effect, cloud lifetime effect and semi-direct effect) (lower panel) from the main analysis. Red color for the posterior distributions and black lines and gray shadings for the prior distribution.

Title Page

Abstract

Introduction

Conclusions

References

Tables

Figures

⏪

⏩

◀

▶

Back

Close

Full Screen / Esc

Printer-friendly Version

Interactive Discussion



A lower and more constrained estimate of climate sensitivity

R. B. Skeie et al.

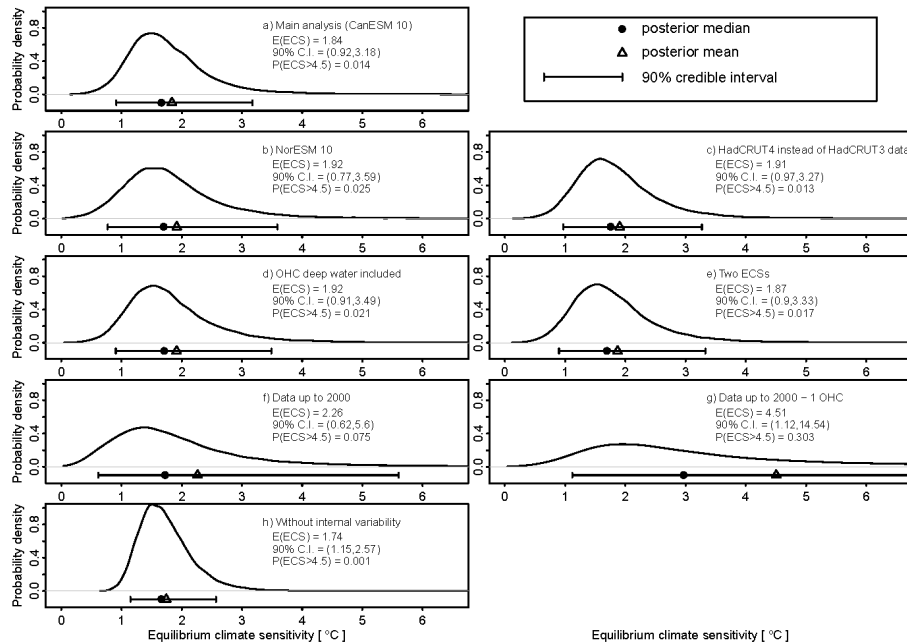


Fig. 2. Posterior distributions for the ECS for different analyses. In **(a)** the main analysis, **(b)** with NorESM data to estimate n_t^{liv} , **(c)** sensitivity test using HadCRUT4 instead of HadCRUT3 data, **(d)** sensitivity test using data for OHC change below 700 m, **(e)** sensitivity test allowing different ECSs in each hemisphere, **(f)** updating the model with data only up to 2000, **(g)** updating the model with data only up to 2000 and using only 1 OHC data series and **(h)** sensitivity test without the long-term internal variability (without the n_t^{liv} term). The estimated mean of ECS, the 90% C.I. and the probability of ECS being larger than 4.5°C are given in the text box of each panel. The 90% C.I. and estimated posterior mean are also indicated in each panel with the black dot and the error bar.

A lower and more constrained estimate of climate sensitivity

R. B. Skeie et al.

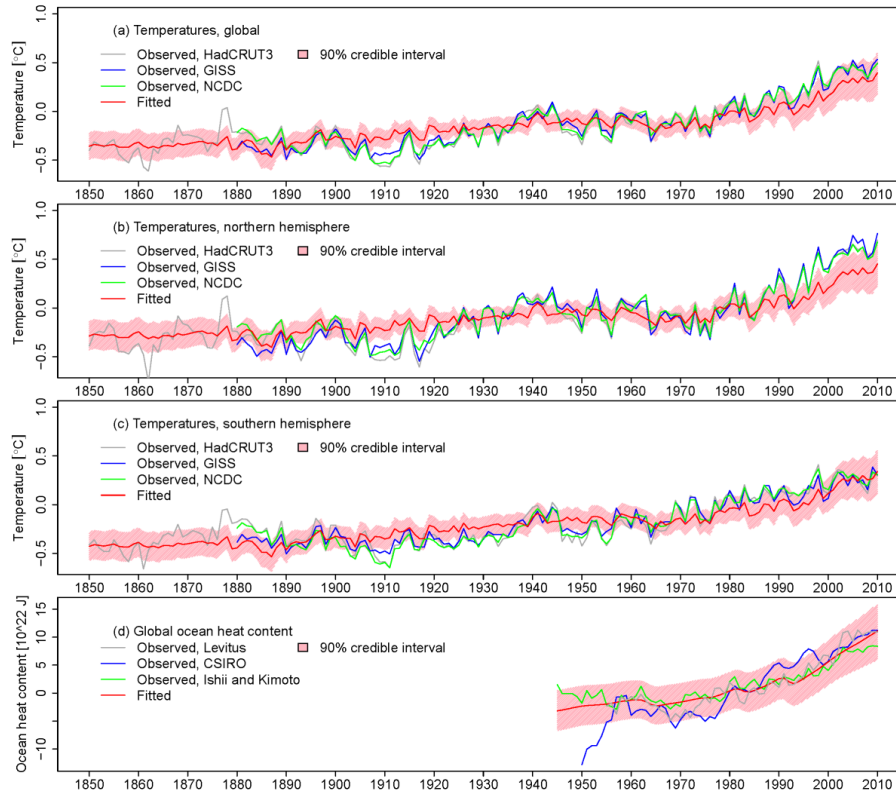


Fig. 3. Observed and fitted (posterior mean) values for the temperature series and the ocean heat content for the main analysis. The shaded areas show the 90 % C.I. for the sum of the two first terms ($m_t(x_{1750:t}, ECS, \theta) + \beta_1 e_t$) at the right side of Eq. (1).

Title Page

Abstract

Introduction

Conclusions

References

Tables

Figures

◀

▶

◀

▶

Back

Close

Full Screen / Esc

Printer-friendly Version

Interactive Discussion



A lower and more constrained estimate of climate sensitivity

R. B. Skeie et al.

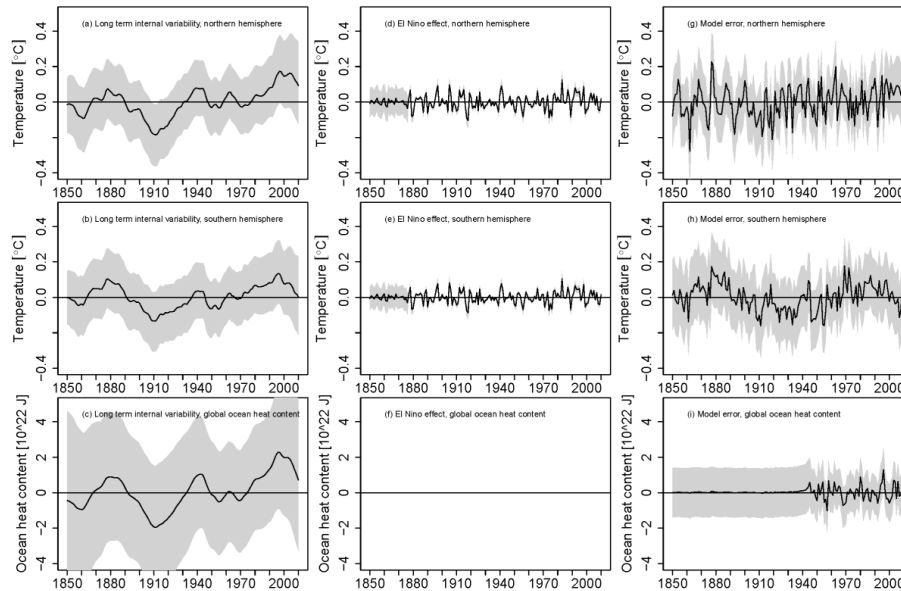


Fig. 4. Posterior estimates of the long-term internal variability term (n_t^{iv} , left column), the ENSO term ($\beta_1 e_t$, middle column) and the model errors (n_t^{m} , right column) for the temperature and ocean heat content.

Title Page

Abstract

Introduction

Conclusions

References

Tables

Figures

◀

▶

◀

▶

Back

Close

Full Screen / Esc

Printer-friendly Version

Interactive Discussion



A lower and more constrained estimate of climate sensitivity

R. B. Skeie et al.

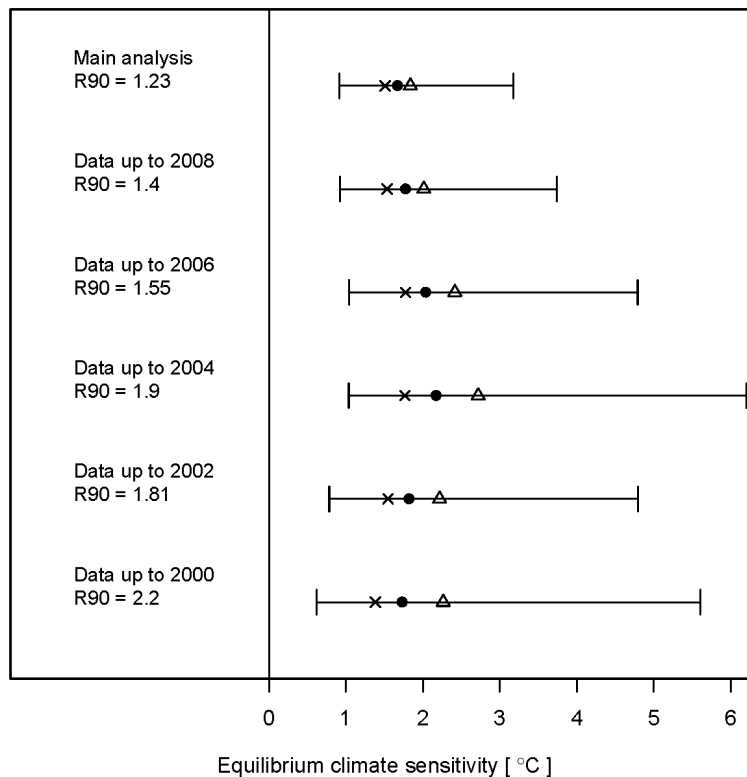


Fig. 5. Posterior means (triangles), medians (dots), modes (crosses), and 90 % credible intervals for estimates of ECS using various data sets updated until between 2000 and 2010 (2 yr intervals). The relative uncertainty measure R90, defined as the width of the 90 % C.I. divided by the posterior mean is also shown.

Title Page

Abstract

Introduction

Conclusions

References

Tables

Figures

◀

▶

◀

▶

Back

Close

Full Screen / Esc

Printer-friendly Version

Interactive Discussion



A lower and more constrained estimate of climate sensitivity

R. B. Skeie et al.

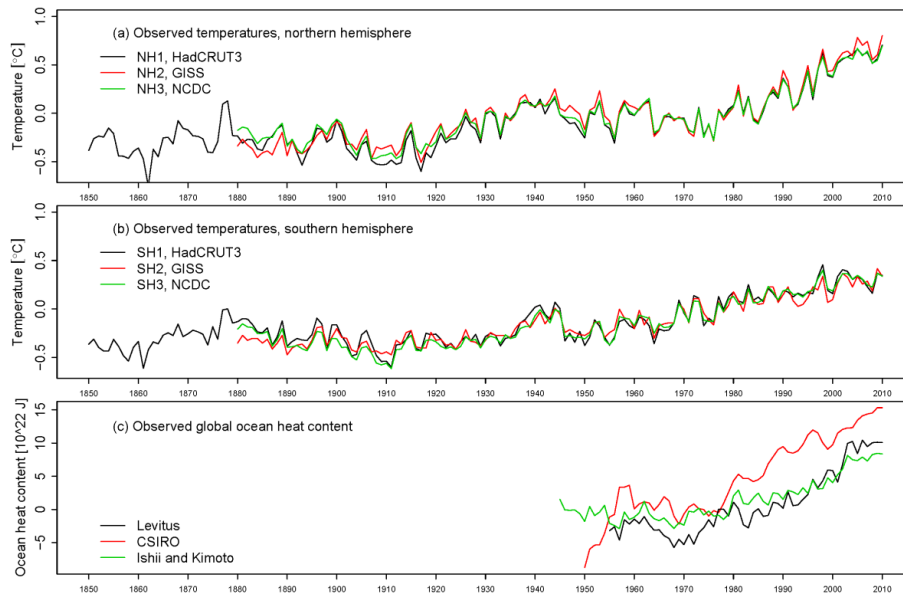


Fig. B1. Annual temperature and ocean heat content data. HadCRUT3, University of East Anglia and the Hadley Centre; GISS, Goddard Institute for Space Studies; NCDC, National Climatic Data Center; CSIRO, Commonwealth Scientific and Industrial Research Organisation.

Title Page

Abstract

Introduction

Conclusions

References

Tables

Figures

◀

▶

◀

▶

Back

Close

Full Screen / Esc

Printer-friendly Version

Interactive Discussion



A lower and more constrained estimate of climate sensitivity

R. B. Skeie et al.

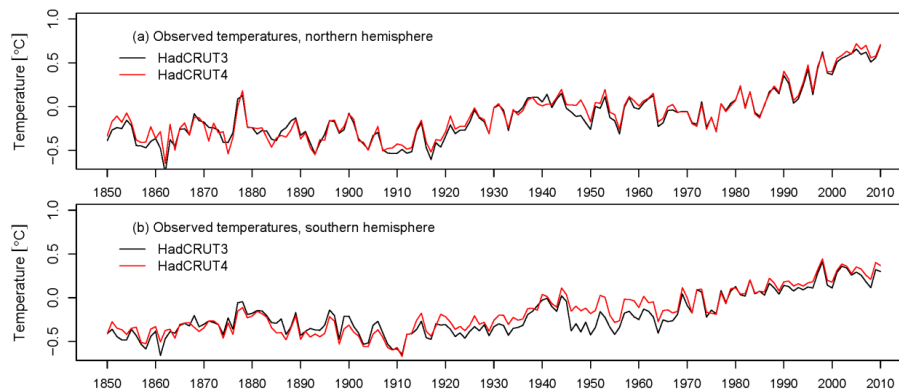


Fig. B2. Annual temperature data. HadCRUT3, University of East Anglia and the Hadley Centre; HadCRUT4, University of East Anglia, King Abdulaziz University and the Hadley Centre.

Title Page

Abstract

Introduction

Conclusions

References

Tables

Figures

◀

▶

◀

▶

Back

Close

Full Screen / Esc

Printer-friendly Version

Interactive Discussion



A lower and more constrained estimate of climate sensitivity

R. B. Skeie et al.

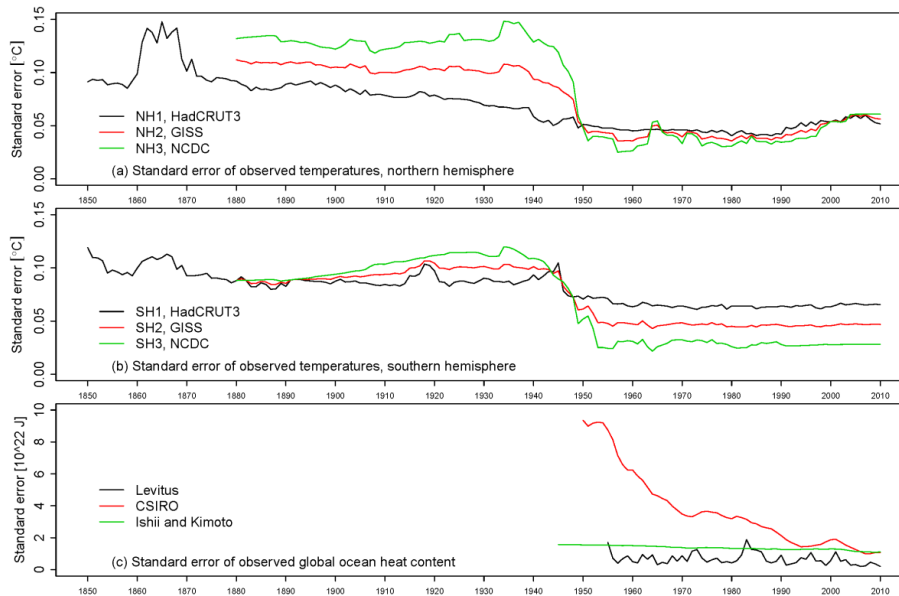


Fig. B3. Reported standard errors of annual temperature and ocean heat content data. The standard errors for the Goddard Institute for Space Studies (GISS) series are simply computed as the middle of the standard errors for the two other series. HadCRUT3, University of East Anglia and the Hadley Centre; NCDC, National Climatic Data Center; CSIRO, Commonwealth Scientific and Industrial Research Organisation.

Title Page

Abstract

Introduction

Conclusions

References

Tables

Figures

◀

▶

◀

▶

Back

Close

Full Screen / Esc

Printer-friendly Version

Interactive Discussion



A lower and more constrained estimate of climate sensitivity

R. B. Skeie et al.

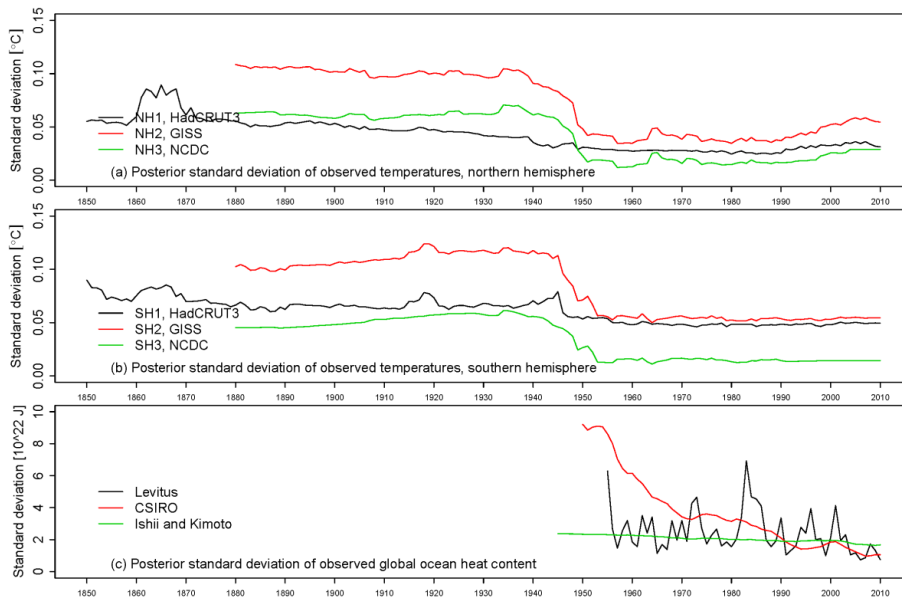


Fig. B4. Posterior estimates of standard deviations of the annual temperature and ocean heat content data.

Title Page

Abstract

Introduction

Conclusions

References

Tables

Figures

◀

▶

◀

▶

Back

Close

Full Screen / Esc

Printer-friendly Version

Interactive Discussion



A lower and more constrained estimate of climate sensitivity

R. B. Skeie et al.

Title Page

Abstract

Introduction

Conclusions

References

Tables

Figures



Back

Close

Full Screen / Esc

Printer-friendly Version

Interactive Discussion

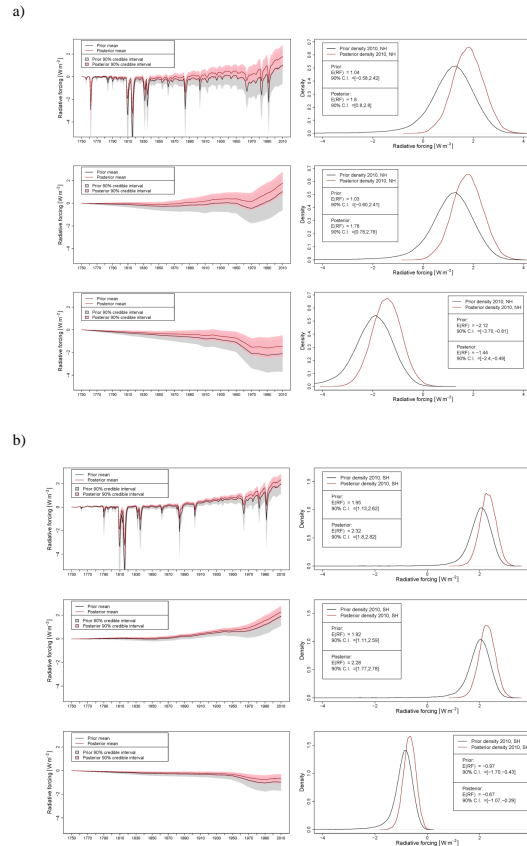


Fig. D1. (a) Prior and posterior distribution of the RF time series and PDF of RF in 2010 for the Northern Hemisphere for total RF (upper panel), anthropogenic RF (middle panel) and total aerosol effect (direct effect, cloud albedo effect, cloud lifetime effect and semi-direct effect) (lower panel) from the main analysis. Red color for the posterior distributions and black lines and gray shadings for the prior distribution; **(b)** as **(a)**, but for the Southern Hemisphere.

A lower and more constrained estimate of climate sensitivity

R. B. Skeie et al.

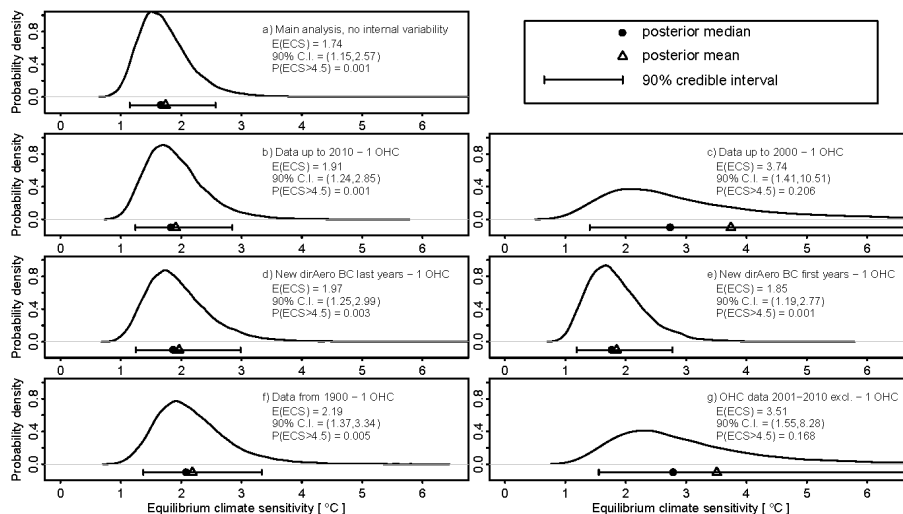


Fig. E1. Posterior distributions for the ECS for analyses where long-term internal variability is not included explicitly in the model (i.e. the term n_t^{liv} is not included in the model) and only one OHC series is used (except for the analysis in panel (a) that is included to show the effect of using three instead of one OHC series). In (a) the main analysis (no long-term internal variability term, 3 OHC series), (b) only one OHC series, (c) use data up to 2000, (d) sensitivity Test 1, changing the direct aerosol BC effect in the latter part of the simulation period, (e) sensitivity Test 2, changing the direct aerosol BC effect in the early part of the simulation period, (f) sensitivity Test 3, using data between 1900 and 2010, (g) sensitivity Test 4, excluding OHC data for the years 2001 to 2010. The estimated mean of ECS, the 90 % C.I. and the probability of ECS being larger than 4.5 °C are given in the text box of each panel. The 90 % C.I. and estimated posterior mean are also indicated in each panel with the black dot and the error bar.

[Title Page](#)
[Abstract](#)
[Introduction](#)
[Conclusions](#)
[References](#)
[Tables](#)
[Figures](#)
[◀](#)
[▶](#)
[◀](#)
[▶](#)
[Back](#)
[Close](#)
[Full Screen / Esc](#)
[Printer-friendly Version](#)
[Interactive Discussion](#)


A lower and more constrained estimate of climate sensitivity

R. B. Skeie et al.

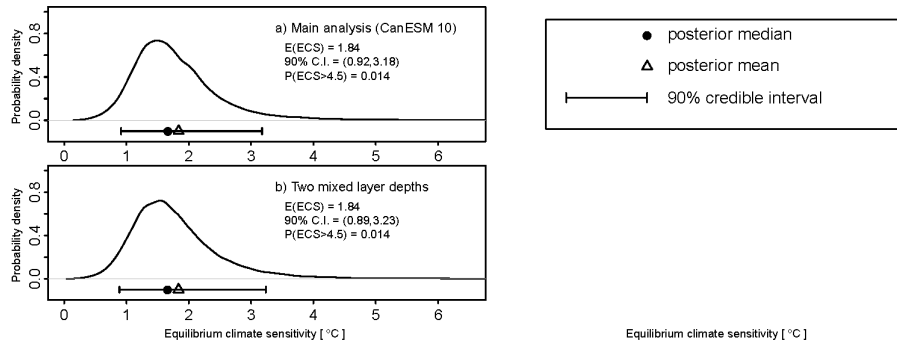


Fig. E2. Posterior distributions for the ECS for **(a)** the main analysis (same as Fig. 2a in the main text), and **(b)** the sensitivity test with two mixed layer depths, one for the Northern Hemisphere (θ_{NH}^M) and one for the Southern Hemisphere (θ_{SH}^M). The estimated mean of ECS, the 90 % C.I. and the probability of ECS being larger than 4.5 °C are given in the text box of each panel. The 90 % C.I. and estimated posterior mean are also indicated in each panel with the black dot and the error bar.

Title Page

Abstract

Introduction

Conclusions

References

Tables

Figures

◀

▶

◀

▶

Back

Close

Full Screen / Esc

Printer-friendly Version

Interactive Discussion



A lower and more constrained estimate of climate sensitivity

R. B. Skeie et al.

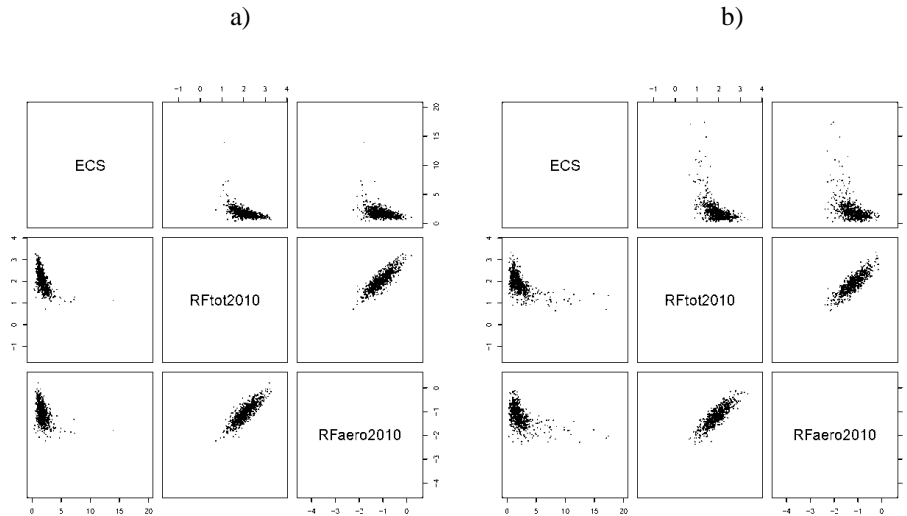


Fig. F1. Pairs plots of samples from the posterior distribution for ECS, total RF in 2010 and total aerosol effect in 2010. In **(a)** the model is updated with data up to 2010, while in **(b)** the model is updated with data up to 2000.

Title Page

Abstract

Introduction

Conclusions

References

Tables

Figures

◀

▶

◀

▶

Back

Close

Full Screen / Esc

Printer-friendly Version

Interactive Discussion



A lower and more constrained estimate of climate sensitivity

R. B. Skeie et al.

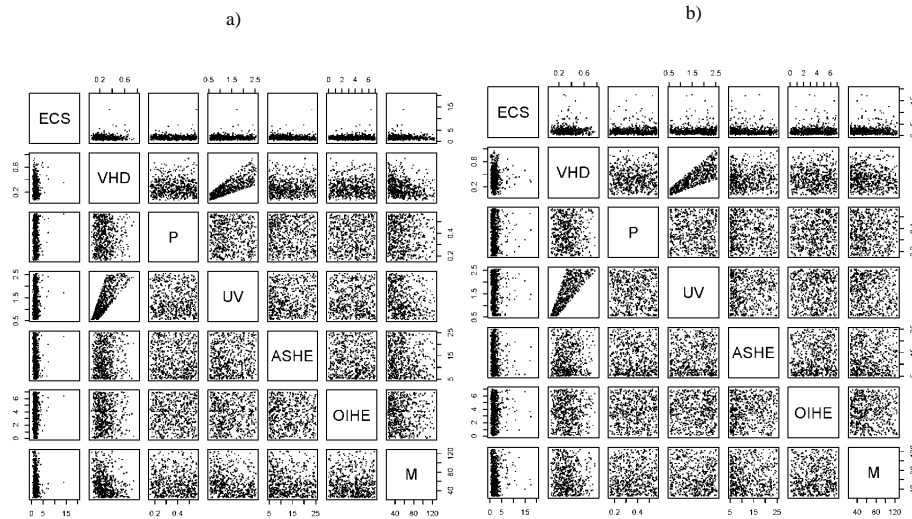


Fig. F2. Pairs plots of samples from the posterior distribution for the model parameters ECS and $\theta = (\theta^{VHD}, \theta^P, \theta^{UV}, \theta^{ASHE}, \theta^{OIHE}, \theta^M)$. In **(a)** the model is updated with data up to 2010, while in **(b)** the model is updated with data up to 2000.

Title Page

Abstract

Introduction

Conclusions

References

Tables

Figures



Back

Close

Full Screen / Esc

Printer-friendly Version

Interactive Discussion

